SKB

TECHNICAL REPORT 87-04

Calculations on HYDROCOIN level 2, case 1 using the GWHRT flow model

Thermal convection and conduction around a field heat transfer experiment

Roger Thunvik
Royal Institute of Technology, Stockholm

March 1987

SVENSK KÄRNBRÄNSLEHANTERING AB
SWEDISH NUCLEAR FUEL AND WASTE MANAGEMENT CO

BOX 5864 S-102 48 STOCKHOLM
TEL 08-665 28 00 TELEX 13108-SKB

CALCULATIONS ON HYDROCOIN LEVEL 2, CASE 1 USING THE GWHRT FLOW MODEL

Thermal convection and conduction around a field heat transfer experiment

Roger Thunvik
Royal Institute of Technology, Stockholm

March 1987

Abstract

The present report presents solutions to Hydrocoin Level 2: Case 1, dealing with thermal convection and conduction around a field heat transfer experiment. Hydrocoin is an international cooperation project to compare different computer models used for describing groundwater flow in geological media. The purpose of the project is to improve the understanding of various strategies for modelling groundwater flow for the safety assessment of final radioactive waste repositories.

The project is structured in three levels. The object of level 1 is to examine the numerical accuracy of the computer models compared. The object of level 2 is to study the capability of computer models to describe in-situ measurements. Level 3 is concerned with sensitivity and uncertainty analysis of groundwater flow.

SUMMARY

The present report presents solutions to Hydrocoin Level 2, Case 1: Thermal convection and conduction around a field heat transfer experiment. The calculations were carried out using the GWHRT-flow model for calculation of coupled flow of groundwater and heat in fractured rock. The model is used for the calculation of groundwater flow at study sites included in the Swedish research program (Swedish Nuclear Fuel Co) for studying the final storage of radioactive waste in hard rock repositories.

The GWHRT-model solves for one, two or three-dimensional saturated-unsaturated flow of water and heat through a fractured rock mass, treated either as a single equivalent continuum or as two overlapping continua. Fluid density is assumed to be dependent of pressure and temperature, while the dynamic viscosity of the fluid is assumed to be dependent of temperature only.

Level 2, Case 1
This case deals with transient thermal convection and conduction around a field heat transfer experiment, in which forced and free convection of water appear to perturb the temperature field due to thermal conduction through the rock. The object of the study is to simulate a heat transfer experiment that was performed in a disused granite quarry in Cornwall. An electrical heater was located in a cased borehole at a mean depth of 44.6 metres. The temperature was recorded at regular time intervals in sixteen boreholes at various distances around the borehole. The water table was generally located close to the surface.

Three different levels were envisaged for the validation exercise: "Steady-state" and transient simulation of the experimental data and simulation with free interpretation of the data. The present study was limited to making some "trial and error" steady-state simulations to establish a set of base parameter values. A few preliminary transient simulations including some variations with regard to anisotropy of the permeability and the natural vertical gradient were also performed.

The heater was represented by a series of point sources whose strengths were chosen such that a uniform heat source was applied to the left hand boundary. A set of preliminary calculations were carried out to establish a set of base parameters. Average parameter values were assumed for rock density and the specific heat of the rock. Permeability was taken to be the highest value and thermal conductivity to be the lowest value of the ranges specified for these parameters. Variations from the base parameter values were checked with regard to anisotropy in the vertical direction and the natural pressure gradient. The agreement with the measured data was fairly good except for in the region close to the heater.

The same parameter setting was also used for a tentative transient simulation. The number of power output intervals as given in the specification report was reduced to 23 non-equidistant intervals (instead of the about 110 intervals as prescribed in the specification document) to make it possible to use larger time steps in the simulation than otherwise would be necessary. Visual inspection of the results showed that the time dependent temperature rises of the three thermometers in the observation boreholes could not be properly described using the parameter setting from the steady-state interpretation of the experimental data.

It could also be noted that the temperature rise profile in the observation borehole was in less agreement with the measured data than for the steady-state simulation. This contradiction may therefore question the definition of the equivalent "steady-state" conditions based on the transient conditions and brings about the fact that the conditions at the quasi-steady state are due to a non-linear process.

No definite conclusions could be drawn from the present study as to whether additional physical phenomena should be included in the conceptual model such as changes in the stress field due to the high temperatures, about 300°C, at the heater. So far only a very small part of the parameter was checked with the present conceptual model. To investigate the problem in a more systematic manner requires that some automatic parameter identification technique be used.

The skewness of the measured temperature rise profiles around the observation borehole suggests that there may be some factor that influences the upward movement of the groundwater close to the borehole. Among possible factors could be mentioned a local inhomogeneity, the natural pressure gradient or some stress effect as mentioned above that influences the upward movement of the groundwater close to the borehole.

Hydrocoin is an international cooperation project to compare different computer models used for describing groundwater flow in geological media. The purpose of the project is to improve the understanding of various strategies for modelling groundwater flow for the safety assessment of final radioactive waste repositories. The project is structured in three levels. The object of level 1 is to examine the numerical accuracy of the computer models compared. The object of level 2 is to study the capability of computer models to describe in-situ measurements. Level 3 is concerned with sensitivity and uncertainty analysis of groundwater flow.

HYDROCOIN Level 2, Case 1
Calculation of thermal convection and conduction around a field heat transfer experiment

Roger Thunvik
Royal Institute of Technology
Stockholm, Sweden

Contents

Introduction

This case deals with transient thermal convection and conduction around a field heat transfer experiment, in which forced and free convection of water appear to perturb the temperature field due to thermal conduction through the rock. The test problem is defined by Hodgkinsonand Herbert (1, 2). The numerical results worked out in the present study are displayed graphically together with some of the measured data.

The object of the present study is to simulate a heat transfer experiment that was performed in a disusedgranite quarry in Cornwall. An electrical heater was located in a cased borehole at a mean depth of 44.6 metres. The temperature was recorded at regular time intervals in sixteen boreholes at various distances around the borehole. The water table was generally located close to the surface.

The energy output from the heater was about 3 kW for the first 273 days, raised to about 9 kW for the next 100 days. The the power was raised to a maximum of 14 kW and progressively reduced and turned off after 2048 days. There were numerous breakdowns of the heater during the five and a half year of operation.

Three different levels were envisaged for the validation exercise: "Steady-state" and transient simulation of the experimental data and simulation with free interpretation of the data. The present study was limited to making some "trial and error" steady-state simulations to establish a set of base parameter values. A few preliminary transient simulations including some variations with regard to anisotropy and the natural vertical gradient were also performed.

Flow model

The numerical model used in the calculations was developed by Thunvik and Braester (3). The following set of equations is used in the calculations

$$\phi\rho^f(c^f + c^r)\, p_{,t} - \phi\rho^f\beta T^f_{,t} - (\rho^f \underline{\underline{k}}_{ij}/\mu\,(p_{,j} - \rho^f g_j) = 0 \qquad (1)$$

$$(\rho C)^*\, T_{,t} - (\lambda^*\, T_{,j})_{,j} + \rho^f C^f q_i T_{,i} + Q = 0 \qquad (2)$$

where ϕ is porosity, ρ^f is fluid density, c^f is fluid compressibility, c^f is rock compressibility, β is coefficient of thermal volume expansion, T is temperature, k_{ij} is the permeability tensor, μ is dynamic viscosity, p is pressure, g is the acceleration of gravity and Q represents the heat source.

In the heat flow equation $(\rho C)^*$ was defined as

$$(\rho C)^* = \phi\lambda^f C^f + (1-\phi)\lambda^r C^r$$

and

$$\lambda^* = \phi\lambda^f + (1-\phi)\,\lambda^r$$

where λ^f is the thermal conductivity.

The flow equations are solved numerically using the Galerkin finite element method. The algebraic system of equations resulting from the Gauss integration over the elements is solved by Gauss elimination using the frontal method.

Boundary and initial conditions

For the fluid flow the boundaries are assumed to be no-flow boundary except on the top boundary, which is assumed to be at constant pressure. In cases where a vertical pressure gradient is applied contant pressure was applied to the bottom boundary according to the assumed gradient.

For the heat flow all boundaries are assumed to be no-flow boundaries except at the boundary section where the heater is applied. Initially, the temperature is set equal to the ambient rock temperature all over the flow domain, i.e. 10.8°C.

Input data

The heater was represented by a series of point sources whose strengthswere chosen such that a uniform heat source was applied to the left hand boundary. Site parameter values as given in the specification of the present problem are presented in Table 1. A set of preliminary calculationswere carried out to establish, by simple trial and error, a set of base parameters (see Table 2).

Average parameter values were assumed for rock density and the specific heat of the rock. Permeability was taken to be the highest value and thermal conductivity to be the lowest value of the ranges specified for these parameters.

The base parameter values used in the calculations are presented in Table 2. Variations from the base parameter values were checked with regard to anisotropy in the vertical direction and the natural pressure gradient.

The parameter values of the variations performed are summarized in Table 4, where S0 and S1 represent solutions for a constant heat source and T1, T2, T3 and T4 represent transient solutions for a time dependent heat source.

The solution was worked out using a mesh of 209 elements and 688 nodes. The mesh used is shown in Figure 1. The radial extent of the flow domain considered was 50 metres and the distance from the ground surface to the bottom of the aquifer was 100 metres. The length of the heater was 4.6 metres and it was located at a mean depth of 44.6 metres.

Table 1. Site parameters

Symbol	Parameter	Value	Unit
λ^r	thermal conductivity	3.3 ± 0.3	$Wm^{-1}K^{-1}$
ρ^r	rock density	2630 ± 25	kgm^{-3}
C^r	rock specific heat	820 ± 100	$Jkg^{-1}K^{-1}$
k	permeability	$3.5\text{-}40\times10^{-14}$	m^2

Table 2. Base parameters values used in the calculations

Symbol	Parameter	Value	Unit
Rock parameters			
ϕ	porosity	0.0001	-
c^r	rock compressibility	0.0	Pa^{-1}
λ^r	thermal conductivity	3.0	$Wm^{-1}K^{-1}$
ρ^r	rock density	2.630	kgm^{-3}
C^r	specific heat capacity	820	$Jkg^{-1}K^{-1}$
k	permeability	4.0×10^{-13}	m^2
Fluid parameters			
c^f	fluid compressibility	10^{-10}	Pa^{-1}
λ^f	thermal conductivity	0.6	$Wm^{-1}K^{-1}$
β	expansion coefficient	$3.85*10^{-4}$	K^{-1}
ρ^f	fluid density	(see function)	kg^{-3}
μ	fluid viscosity	(see function)	$kgm^{-1}s^{-1}$
C^f	specific heat capacity	4180	$Jkg^{-1}K^{-1}$
λ^*	average value of thermal thermal conductivity		$Wm^{-1}K^{-1}$
$(\rho C)^*$	average value of density times specific heat		

The following function for density was used in the calculations (2)

$$\rho(T) = \rho_R \exp(y_\rho(a_1 + y_\rho(a_2 + y_\rho(a_3 + y_\rho(a_4 + y_\rho a_5)))))$$

where

$$y_\rho = (T_\rho/(T + T_o + 273.2) - 1)^{1/3}$$

and the following function for viscosity was used (2)

$$\mu(T) = \mu_R \exp(b_1 y_\mu + y_\mu^3(b_2 + y_\mu^3(b_3 + b_4 y_\mu + b_5 y_\mu^{24})))$$

where

$$y_\mu = (T_\mu/(T + T_o + 273.2) - 1)^{1/3}$$

The various constants appearing in these expressions (a_n, b_n, ρ_R, μ_R, T_ρ, T_μ) are given in Table 3.

Table 3. Parameters appearing in the expressions for the temperature dependence of the density and viscosity of water

Parameter	Value
ρ_R	315.5
a_1	2.0233201
a_2	-0.49864401
a_3	-1.0282498
a_4	0.9465529
a_5	-0.30178144
T_ρ	647.30
μ_R	$39.06*10^{-6}$
b_1	1.5537
b_2	-0.20276
b_3	1.9107
b_4	-0.63486
b_5	0.0050468
T_μ	647.27

Table 4. Parameter settings [1)]

Setting	k_{11}	k_{22}	Natural pressure gradient
S0	1.0	1.0	0.000
S1	1.0	1.0	0.025
T1	1.0	1.0	0.025
T2	1.0	1.0	0.000
T3	1.0	5.0	0.000
T4	1.0	5.0	0.025

1) $k_x = k_{11} * k, \quad k_y = k_{22} * k$

Results

The best steady-state solution was obtained for isotropic flow conditions and a natural vertical pressure gradient of 0.025. This judgment was simply based upon visual inspection of the graphical display of the temperature rise profile along the obervation borehole located at r=2.83 metres (see Figure 4). The agreement with the measured data is fairly good except for in the region close to the heater.

The same parameter setting was also used for a tentative transient simulation. The number of power output intervals as given in the specification report was reduced into 23 non-equidistant intervals to make it possible to use larger time steps in the simulation than otherwise would be necessary (see Figure 6). Visual inspection of the results shows that the time dependent temperature rises of the three thermometers in the observation boreholes could not be properly described using the parameter setting from the steady-state interpretation of the experimental data.

It could also be noted that the temperature rise profile in the observation borehole was in less agreement with the measured data than for the steady-state simulation (Figure 4). This contradiction may therefore question the definition of the equivalent "steady-state" conditions based on the transient conditions and brings about the fact that the conditions at the quasi-steady state are due to a non-linear process.

The results for isotropic permeability and zero natural vertical gradient showed less agreement between the numerical and the recorded data in comparison with the results for a natural gradient of 0.025. The calculated temperature rise is too high for the middle thermometer and slightly too low for the top thermometer (see Figure 12). The temperature rise profile at quasi-steady state is shifted downwards in comparison with the measured data (see Figure 13).

The results for vertical anisotropy and zero natural vertical gradient showed better agreement at quasi-steady state than for isotropic permeability and a gradient of 0.025 (Figure 18). The calculated time dependent temperature rise of the top thermometer is in rather poor agreement with the measured data and the behaviour is characterized by exaggerated temperature responses to the changes of the power output (see Figure 17). Moreover, the curves for the middle and top thermometers are crossing one another after about 1500 days. The results for both vertical anisotropy and an imposed vertical gradient were even worse than for the previous case.

No definite conclusions could be drawn from the present study as to whether additional physical phenomena should be included in the conceptual model such as changes in the stress field due to the high temperatures, about 300°C, at the heater. So far only a very small part of the parameter space has been checked for the present conceptual model.

To investigate the problem in a more systematic manner requires that some objective criteria be established. Furthermore, in order to study the effects of several parameters simultaneously, it becomes necessary to apply some automatic technique for the parameter search so that the simultaneous interaction of several parameters could be studied in an objective way.

The skewness of the measured temperature rise profiles around the observation borehole suggests that there may be some factor that influences the upward movement of the groundwater close to the borehole. Among possible factors could be mentioned a local inhomogeneity, the natural pressure gradient or some stress effect as mentioned above that influences the upward movement of the groundwater close to the borehole.

References

1. Hodgkinson, D. and Herbert Alan, 1985, Specification of a test problem for Hydrocoin Level 2 Case 1: Thermal convection and conduction around a field heat transfer experiment, AERE -R - 11627, DOE/RW/85.028.

2. Hodgkinson, D. and Herbert Alan, 1984, Specification of a test problem for Hydrocoin Level 2 Case 1: Thermal convection and conduction around a field heat transfer experiment, AERE -R - 11627, DOE/RW/84, January 1985.

3. Thunvik,R. and Braester, C., 1980, Hydrothermal conditions around a radioactive waste repsitory, Part 1 - A mathematical model for the flow of groundwater and heat in fracture rock, part 2 - Numerical solutions, Part 3 - Numerical solutions for anisotropy, SKBF-KBS-TR:80-19.

Figures

---------- Case T1 ----------

Figure 8. Time dependent power output from the heater. Permeability is isotropic and the natural vertical pressure gradient is 0.025.

Figure 9. Time dependent temperature rises of the top (z=9.4 m), middle (z=1.0 m) and bottom (z=-7.4 m) resistance thermometers in the observation borehole (r=2.83 m). Permeability is isotropic and the natural vertical pressure gradient is 0.025.

Figure 10. Temperature rise profile at the observation borehole (r=2.83 m). Solid line denotes simulated value and asterisks denote measured values. Permeability is isotropic and the natural vertical pressure gradient is 0.025.

Figure 11. Temperature contour plot of the area around the heater for transient solution. Permeability is isotropic and the natural vertical pressure gradient is 0.025.

Figure 12. Flow velocity plot for transient solution after 1475 days. Permeability is isotropic and the natural vertical pressure gradient is 0.025.

---------- Case T2 ----------

Figure 13. Time dependent power output from the heater. Permeability is isotropic and the natural vertical pressure gradient is 0.000.

Figure 14. Time dependent temperature rises of the top (z=9.4 m), middle (z=1.0 m) and bottom (z=-7.4 m) resistance thermometers in the observation borehole (r=2.83 m). Permeability is isotropic and the natural vertical pressure gradient is 0.000.

Figure 15. Temperature rise profile at the observation borehole (r=2.83 m). Solid line denotes simulated value and asterisks denote measured values. Permeability is isotropic and the natural vertical pressure gradient is 0.000.

Figure 16. Temperature contour plot of the area around the heater for transient solution. Permeability is isotropic and the natural vertical pressure gradient is 0.000.

Figure 17. Flow velocity plot for transient solution after 1475 days. Permeability is isotropic and the natural vertical pressure gradient is 0.000.

---------- Case T3 ----------

Figure 18. Time dependent power output from the heater. Permeability is vertically anisotropic and the natural vertical pressure gradient is 0.000.

Figure 19. Time dependent temperature rises of the top (z=9.4 m), middle (z=1.0 m) and bottom (z=-7.4 m) resistance thermometers in the observation borehole (r=2.83 m). Permeability is vertically anisotropic and the natural vertical pressure gradient is 0.000.

Figure 20. Temperature rise profile at the observation borehole (r=2.83 m). Solid line denotes simulated value and asterisks denote measured values. Permeability is vertically anisotropic and the natural vertical pressure gradient is 0.000.

Figure 21. Temperature contour plot of the area around the heater for transient solution. Permeability is vertically anisotropic and the natural vertical pressure gradient is 0.000.

Figure 22. Flow velocity plot for transient solution after 1475 days. Permeability is vertically anisotropic and the natural vertical pressure gradient is 0.000.

---------- Case T4 ----------

Figure 23. Time dependent power output from the heater. Permeability is vertically anisotropic and the natural vertical pressure gradient is 0.025.

Figure 24. Time dependent temperature rises of the top (z=9.4 m), middle (z=1.0 m) and bottom (z=-7.4 m) resistance thermometers in the observation borehole (r=2.83 m). Permeability is vertically anisotropic and the natural vertical pressure gradient is 0.025.

Figure 25. Temperature rise profile at the observation borehole (r=2.83 m). Solid line denotes simulated value and asterisks denote measured values. Permeability is vertically anisotropic and the natural vertical pressure gradient is 0.025.

Figure 26. Temperature contour plot of the area around the heater for transient solution. Permeability is vertically anisotropic and the natural vertical pressure gradient is 0.025.

Figure 27. Flow velocity plot for transient solution after 1475 days. Permeability is vertically anisotropic and the natural vertical pressure gradient is 0.025.

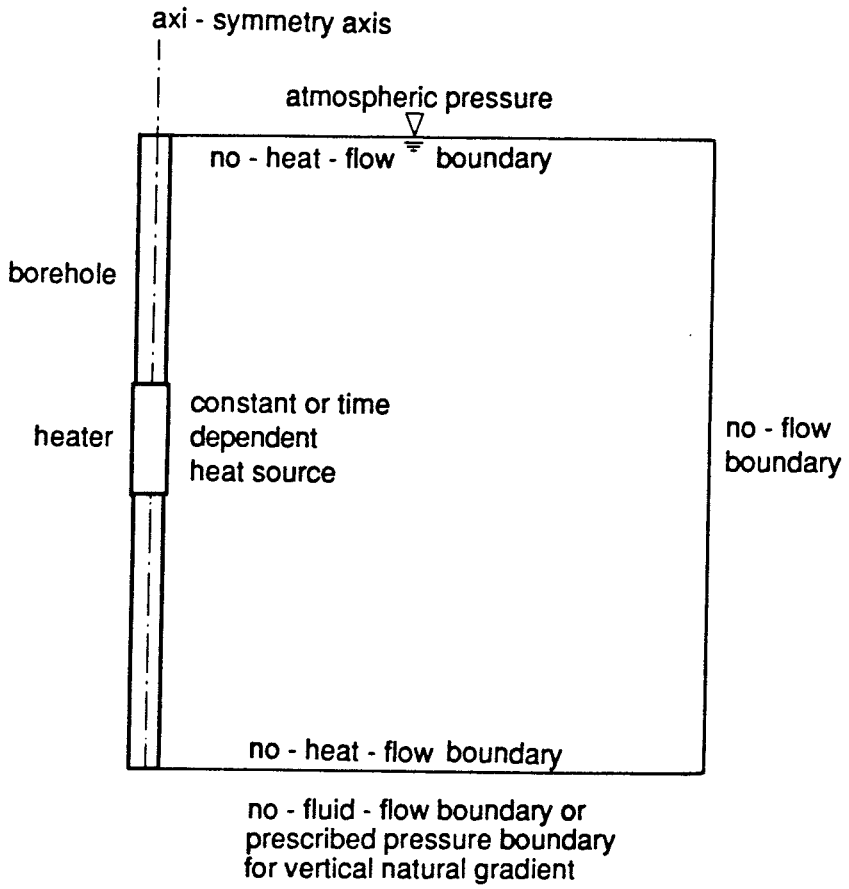

Figure 1. Schematic illustration of the flow problem

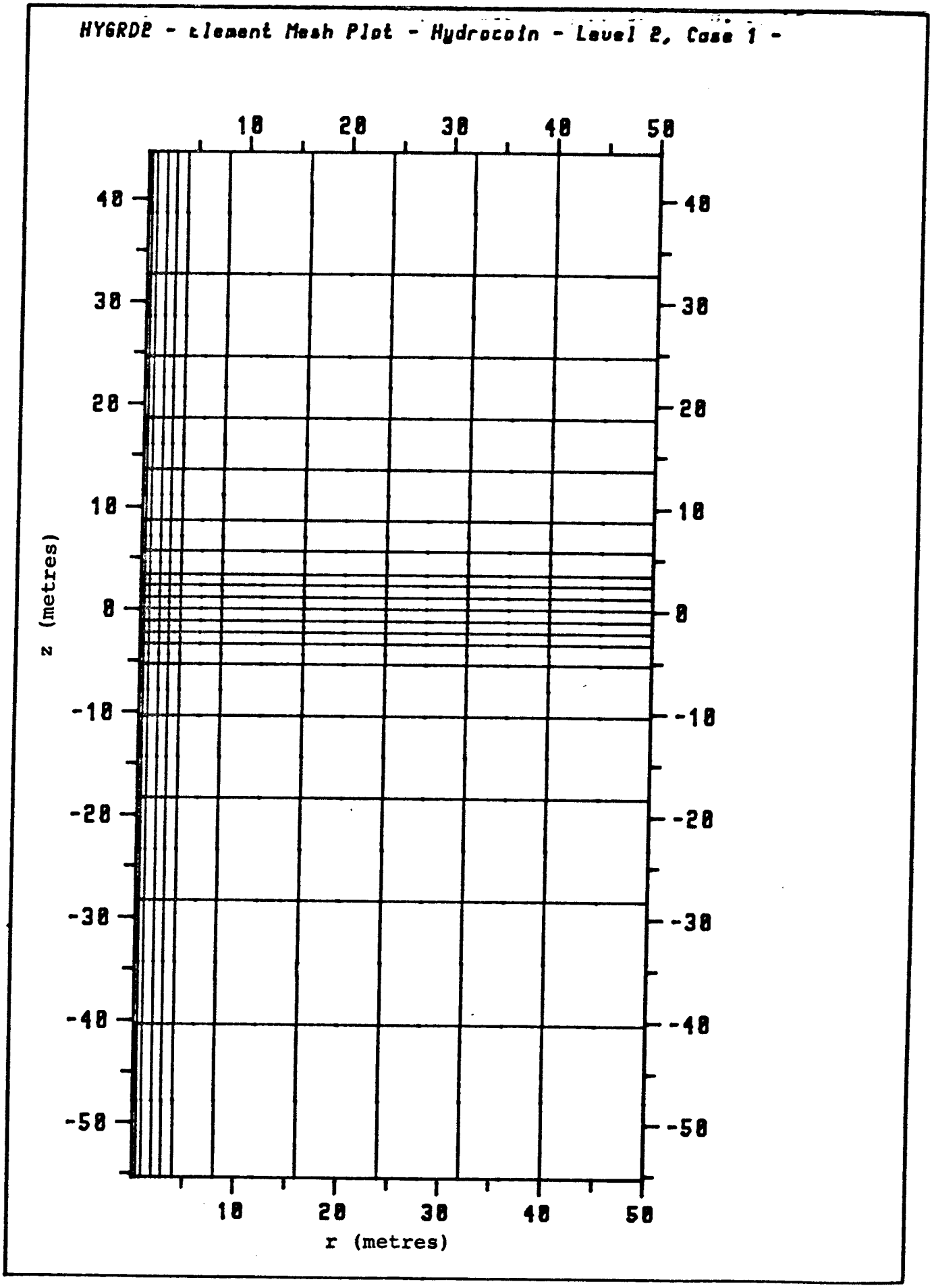
HYGRDE - Element Mesh Plot - Hydrocoin - Level 2, Case 1 -
10
20
30
40
50
40
30
20
10
0
-10
-20
-30
-40
-50
z (metres)
r (metres)

Figure 2.

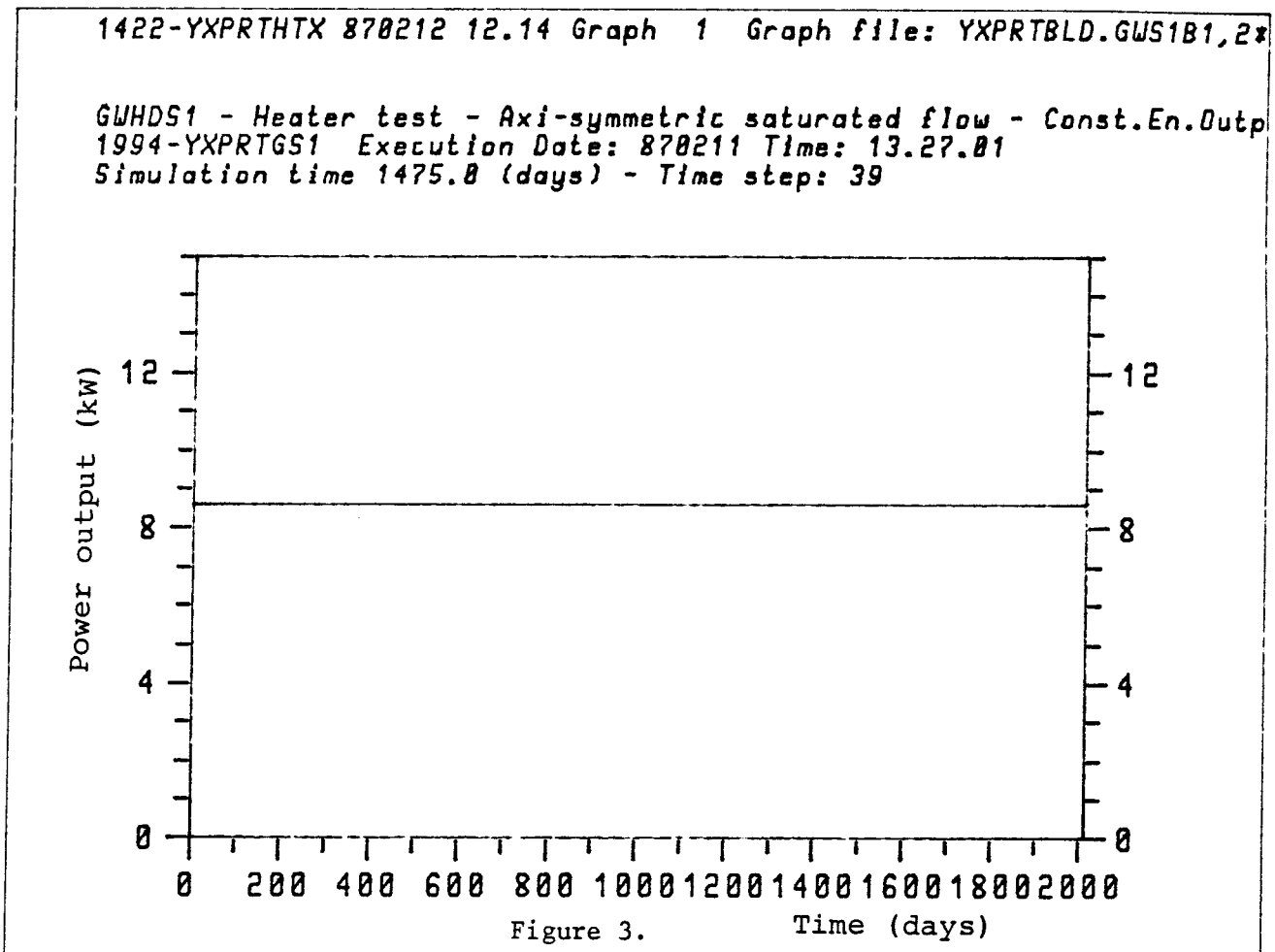

Figure 3.

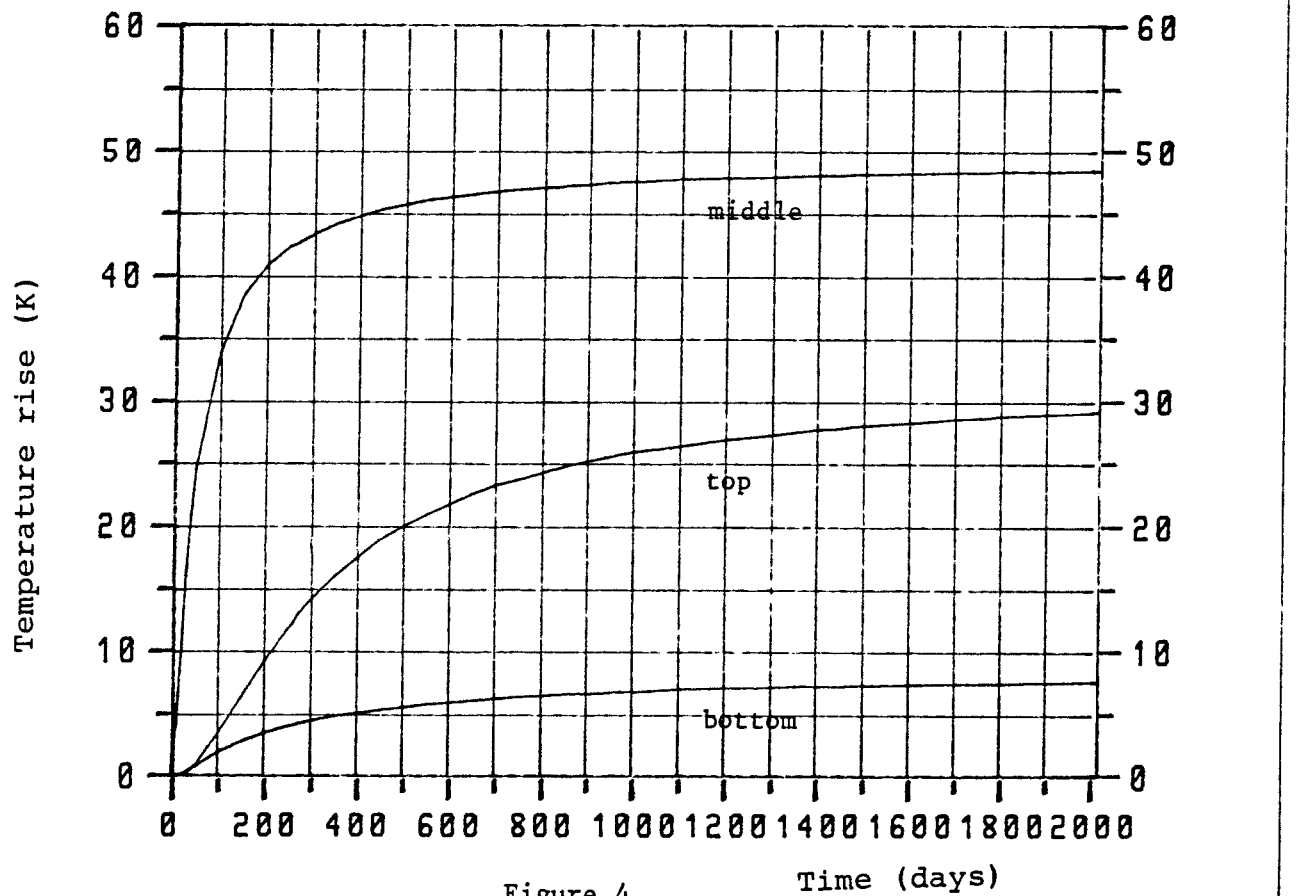

Figure 4.

985-YXPRTHTX 870212 8.54 Graph 1 Graph file: YXPRTBLD.WS1B1,2

GWHDS1 - Heater test - Axi-symmetric saturated flow - Const.En.Dutp
1994-YXPRTGS1 Execution Date: 870211 Time: 13.27.01
Simulation time 1475.0 (days) - Time step: 39

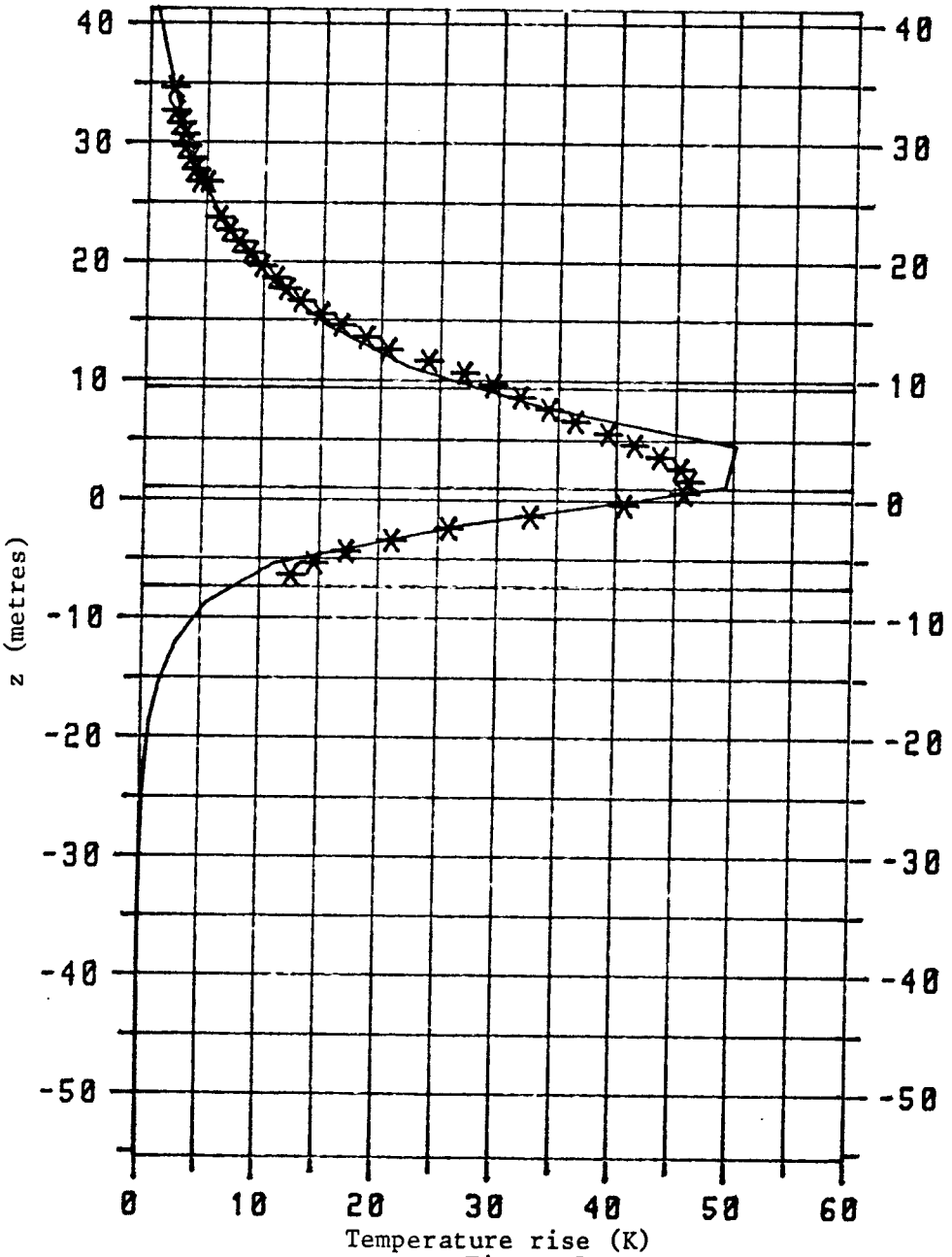

Figure 5.

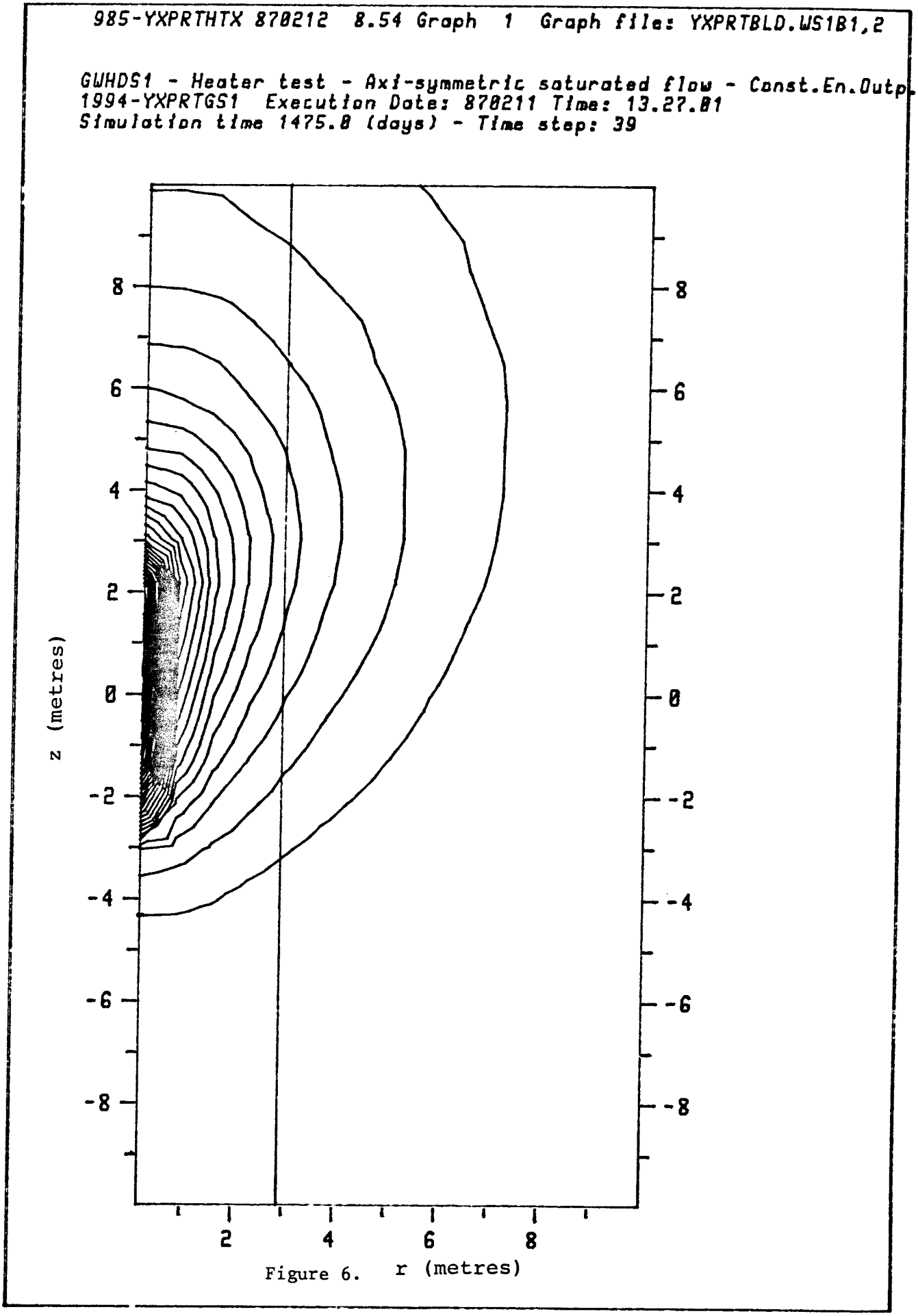
985-YXPRTHTX 870212 8.54 Graph 1 Graph file: YXPRTBLD.WS1B1,2
GWHDS1 - Heater test - Axi-symmetric saturated flow - Const.En.Outp.
1994-YXPRTGS1 Execution Date: 870211 Time: 13.27.81
Simulation time 1475.8 (days) - Time step: 39
z (metres)
8
6
4
2
0
-2
-4
-6
-8
2
4
6
8
r (metres)

Figure 6.

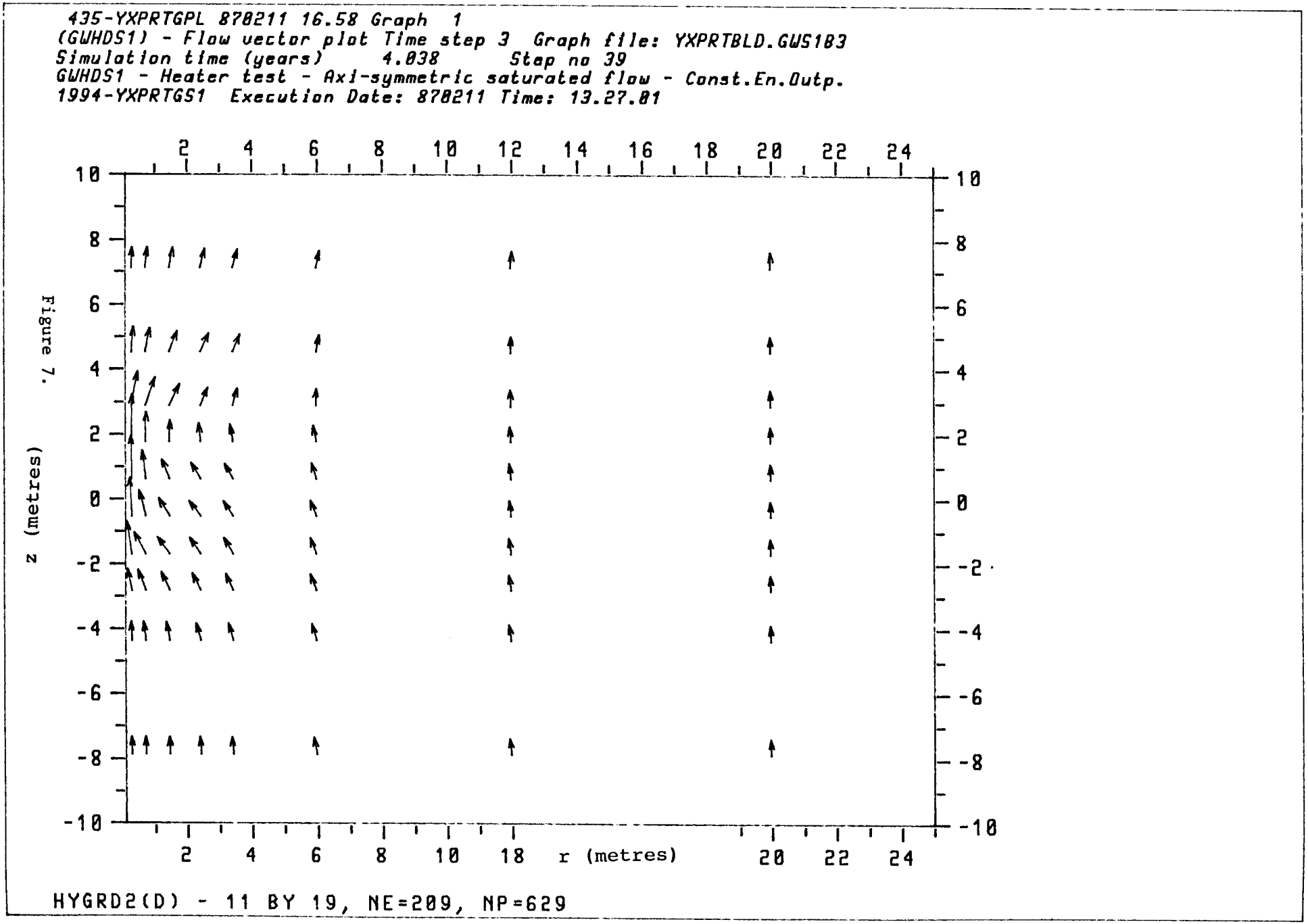
435-YXPRTGPL 870211 16.58 Graph 1
(GWHDS1) - Flow vector plot Time step 3 Graph file: YXPRTBLD.GWS183
Simulation time (years) 4.038 Step no 39
GWHDS1 - Heater test - Axi-symmetric saturated flow - Const.En.Outp.
1994-YXPRTGS1 Execution Date: 870211 Time: 13.27.01
z (metres)
r (metres)
HYGRD2(D) - 11 BY 19, NE=209, NP=629

Figure 7.

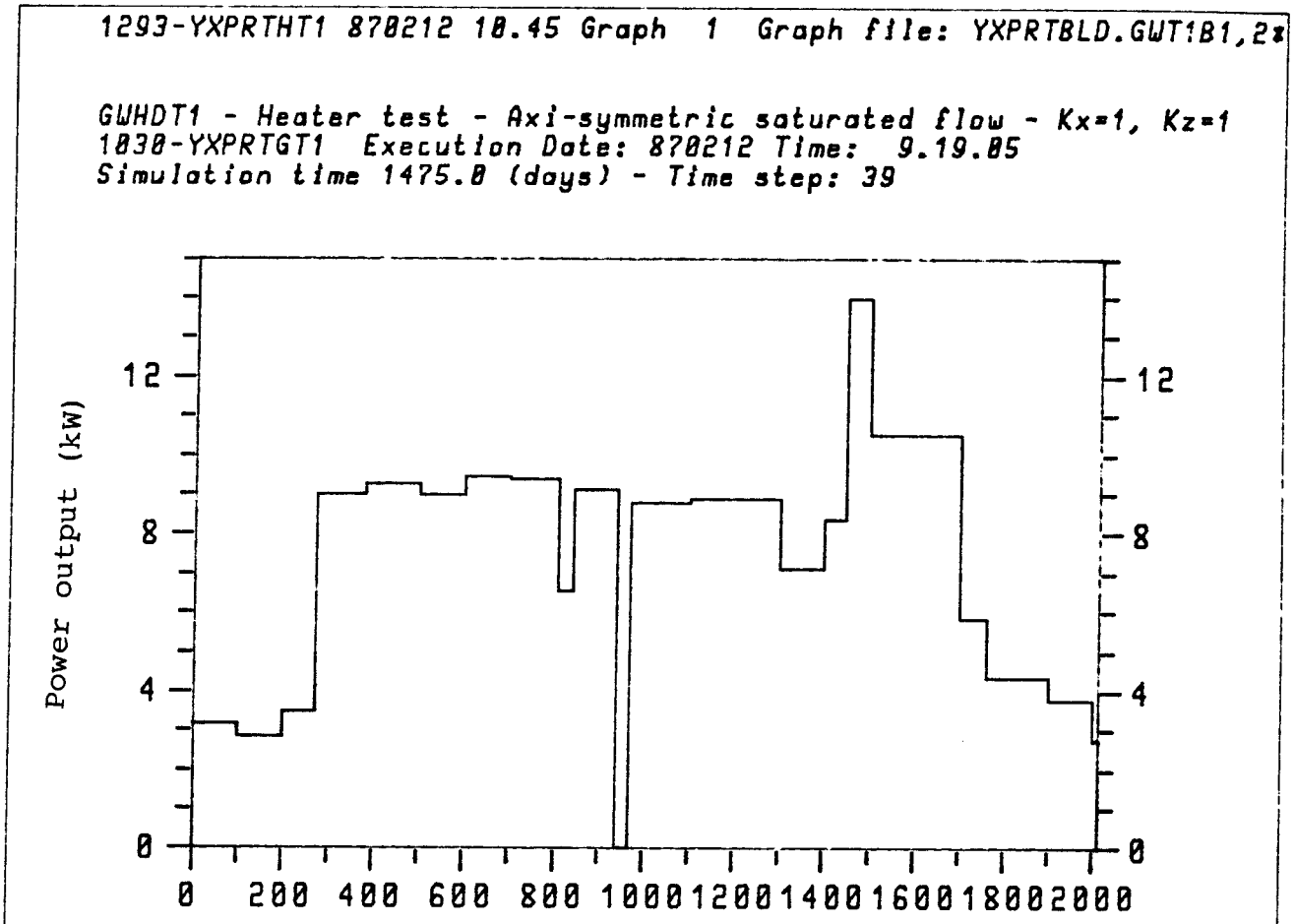

Figure 8.

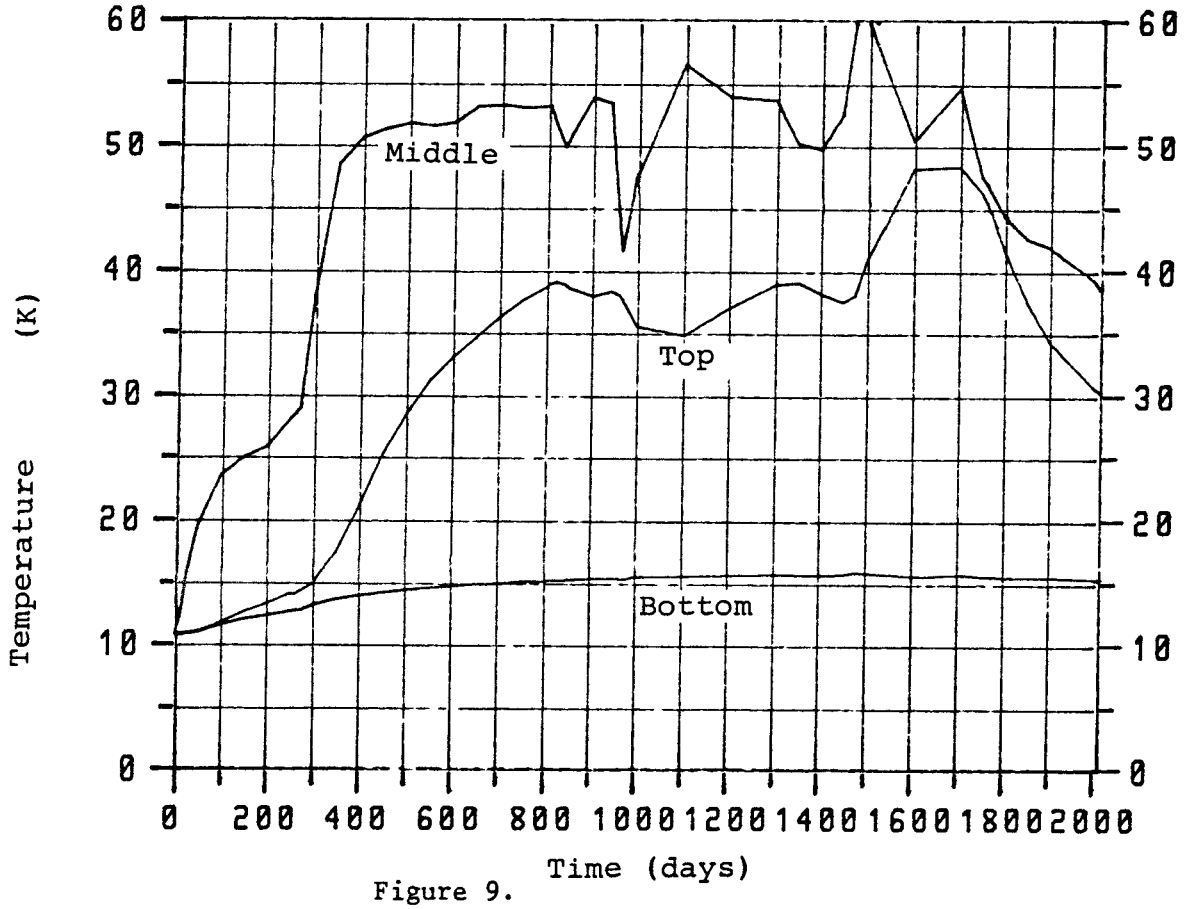

Figure 9.

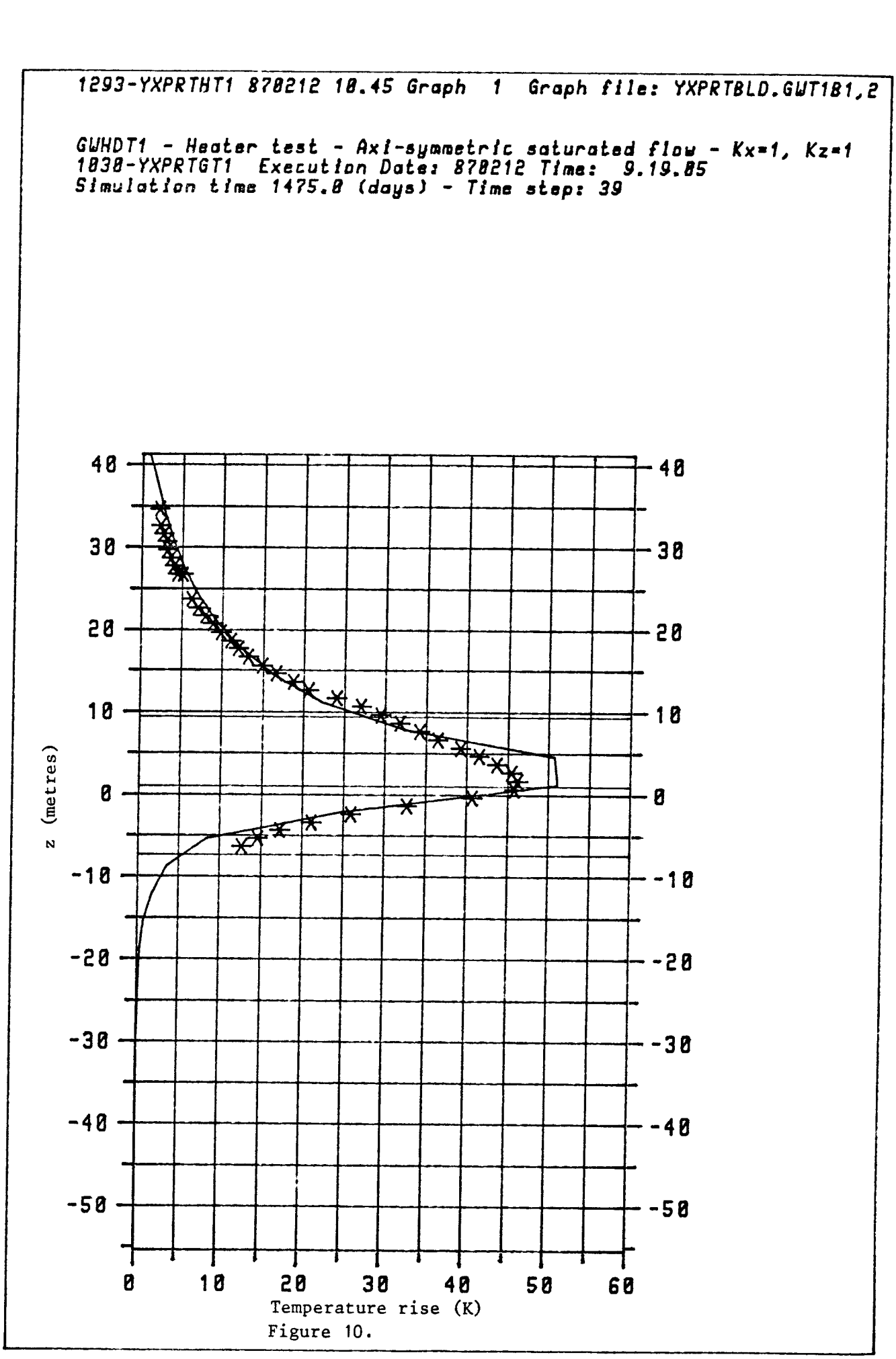
1293-YXPRTHT1 870212 10.45 Graph 1 Graph file: YXPRTBLD.GWT1B1,2
GWHDT1 - Heater test - Axi-symmetric saturated flow - Kx=1, Kz=1
1030-YXPRTGT1 Execution Date: 870212 Time: 9.19.85
Simulation time 1475.0 (days) - Time step: 39
z (metres)
40
30
20
10
0
-10
-20
-30
-40
-50
0
10
20
30
40
50
60
Temperature rise (K)

Figure 10.

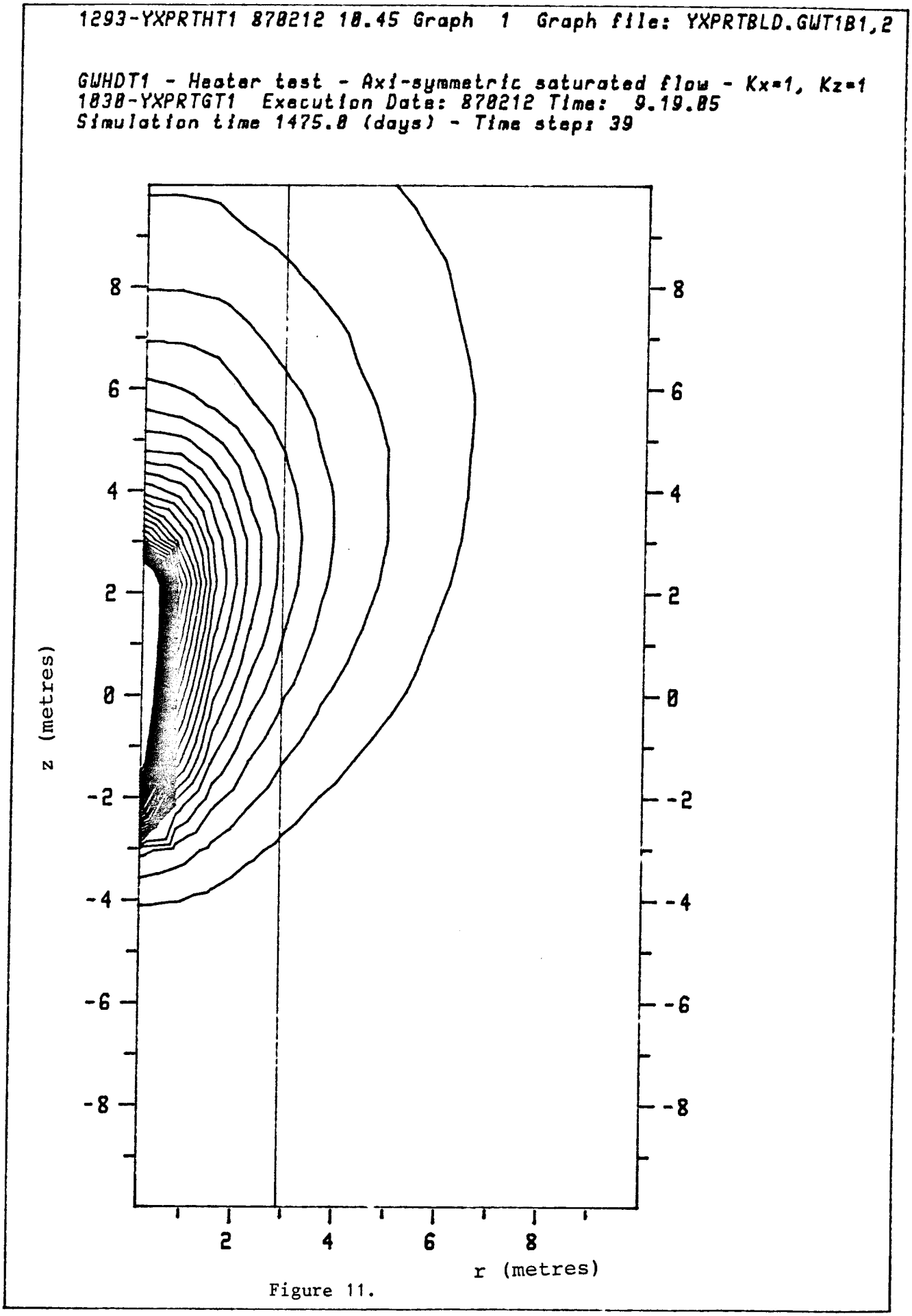
1293-YXPRTHT1 870212 10.45 Graph 1 Graph file: YXPRTBLD.GWT1B1,2
GWHDT1 - Heater test - Axi-symmetric saturated flow - Kx=1, Kz=1
1838-YXPRTGT1 Execution Date: 870212 Time: 9.19.05
Simulation time 1475.0 (days) - Time step: 39
z (metres)
r (metres)
8
6
4
2
0
-2
-4
-6
-8
2
4
6
8

Figure 11.

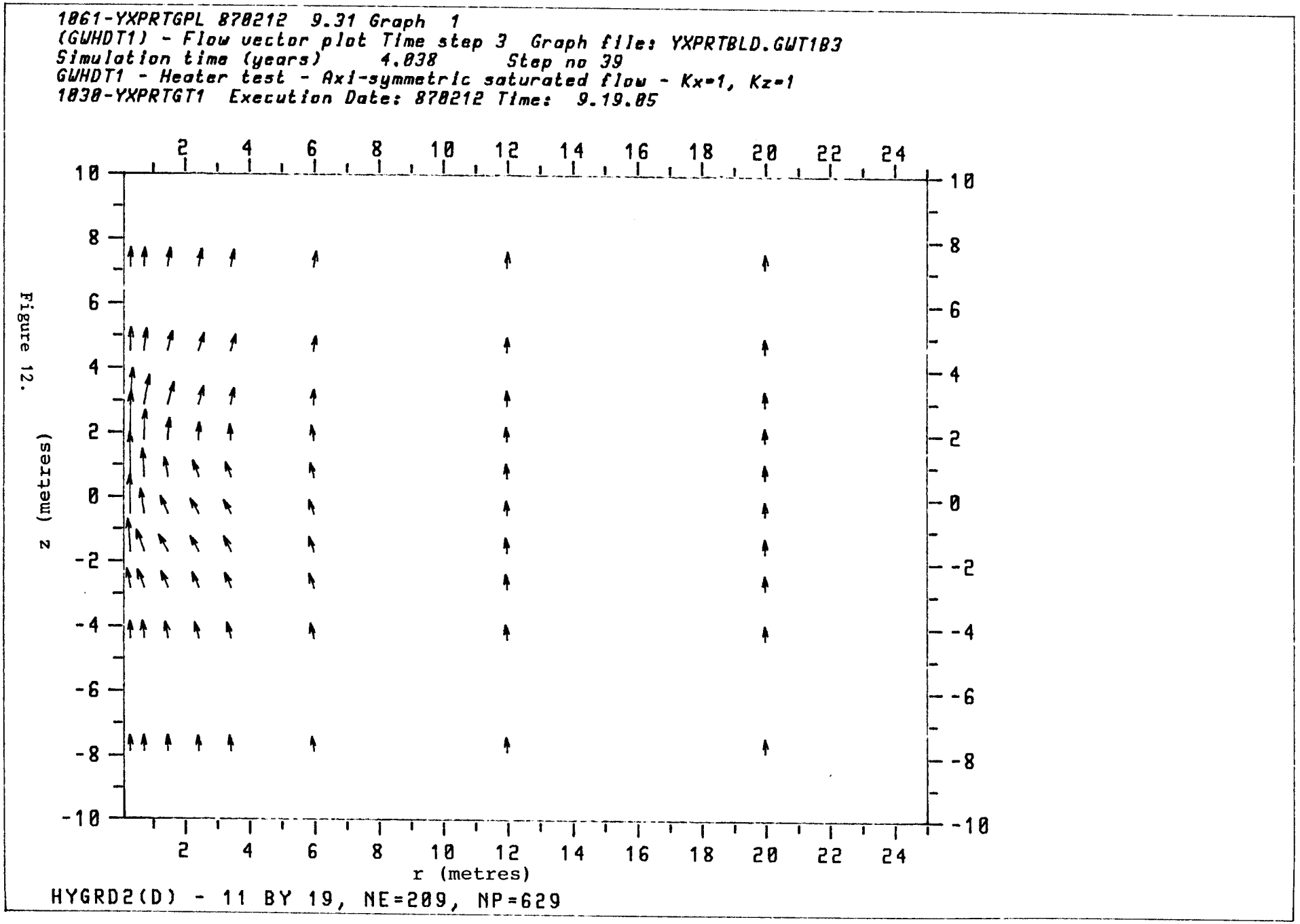
1061-YXPRTGPL 870212 9.31 Graph 1
(GWHDT1) - Flow vector plot Time step 3 Graph file: YXPRTBLD.GUT1B3
Simulation time (years) 4.038 Step no 39
GWHDT1 - Heater test - Axi-symmetric saturated flow - Kx=1, Kz=1
1030-YXPRTGT1 Execution Date: 870212 Time: 9.19.05
2 4 6 8 10 12 14 16 18 20 22 24
10 8 6 4 2 0 -2 -4 -6 -8 -10
z (metres)
r (metres)
HYGRD2(D) - 11 BY 19, NE=209, NP=629

Figure 12.

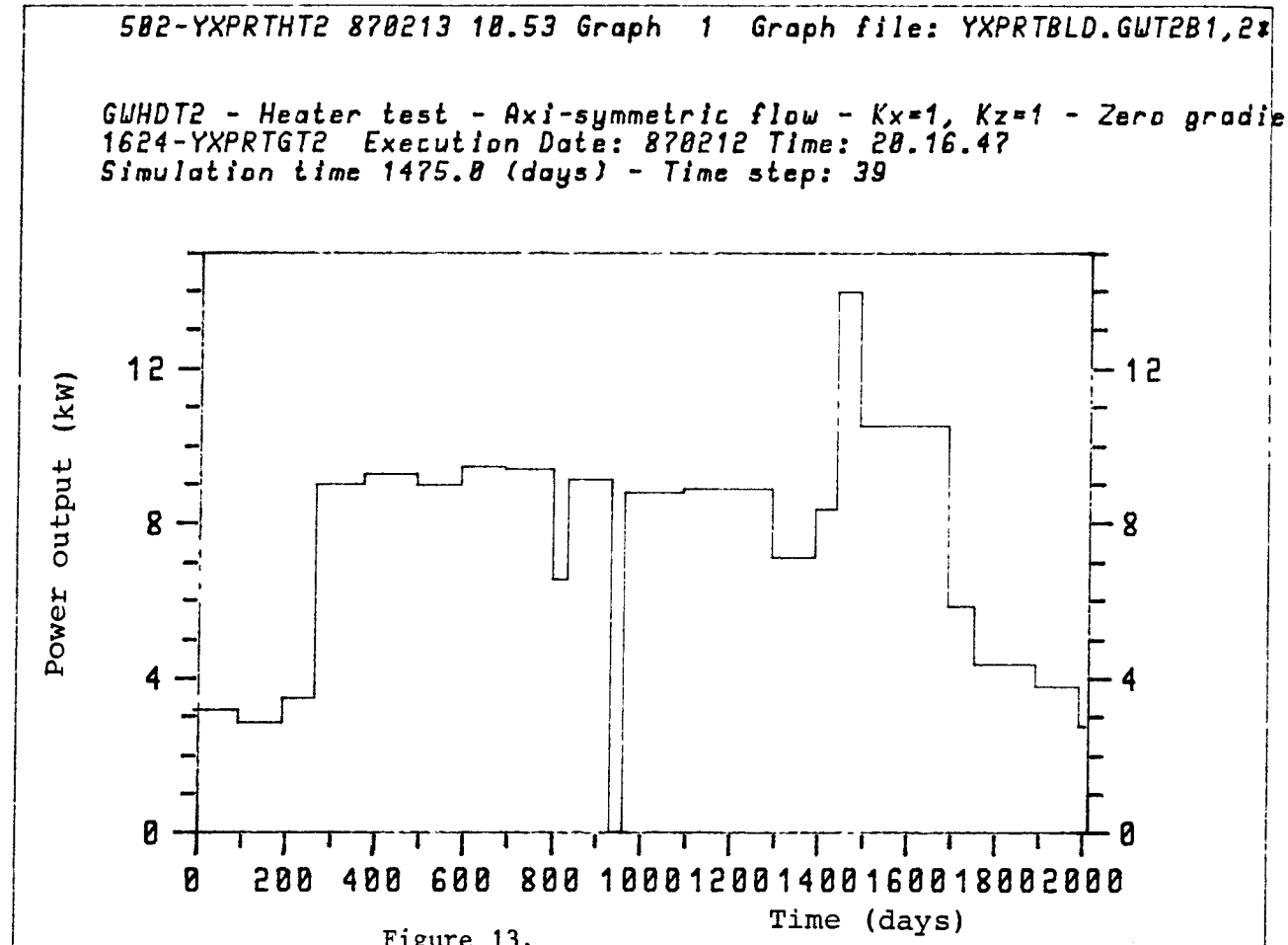

Figure 13.

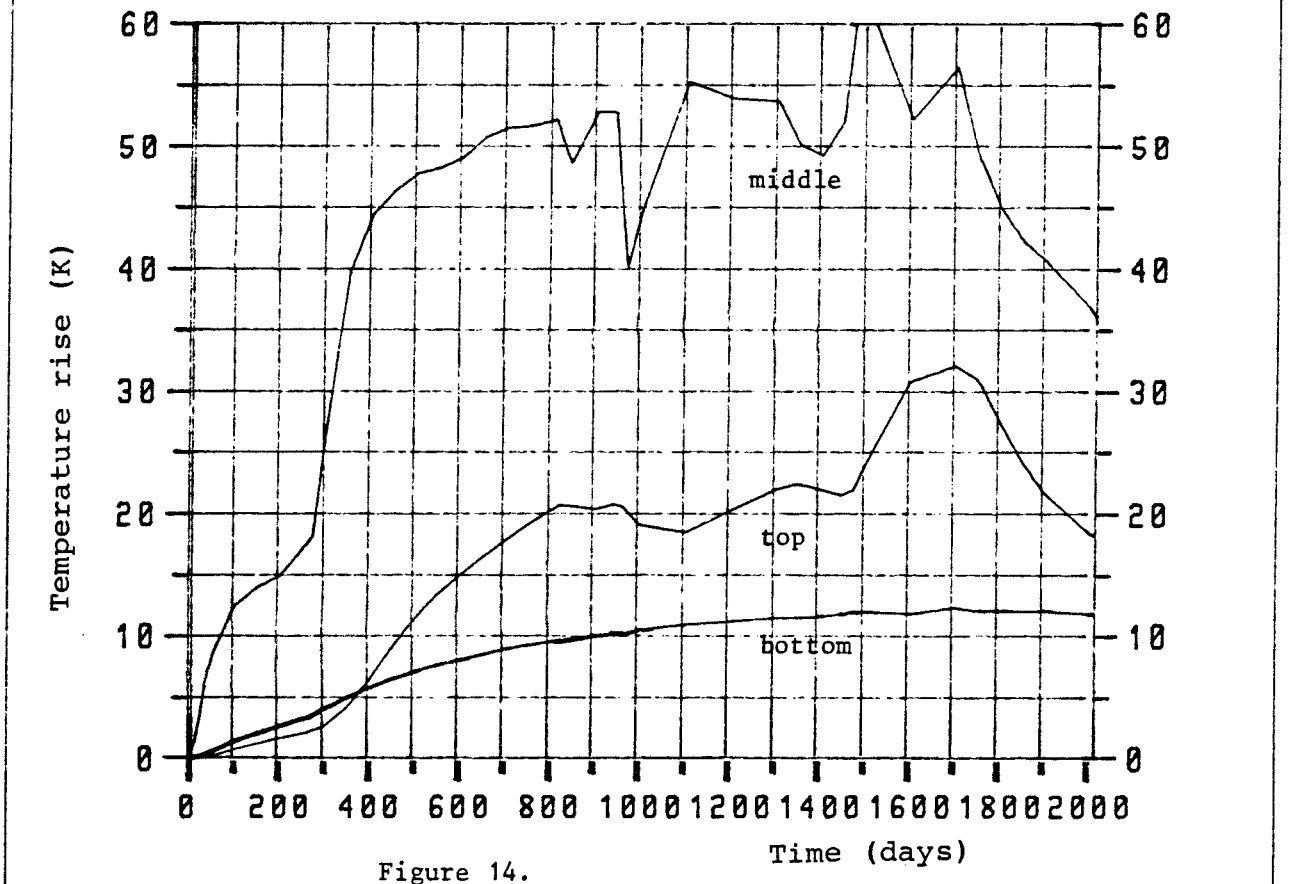

Figure 14.

602-YXPRTHT2 870213 11.59 Graph 1 Graph file: YXPRTBLD.GWT2B1,2

GWHDT2 - Heater test - Axi-symmetric flow - Kx=1, Kz=1 - Zero gradi
1624-YXPRTGT2 Execution Date: 870212 Time: 20.16.47
Simulation time 1475.0 (days) - Time step: 39

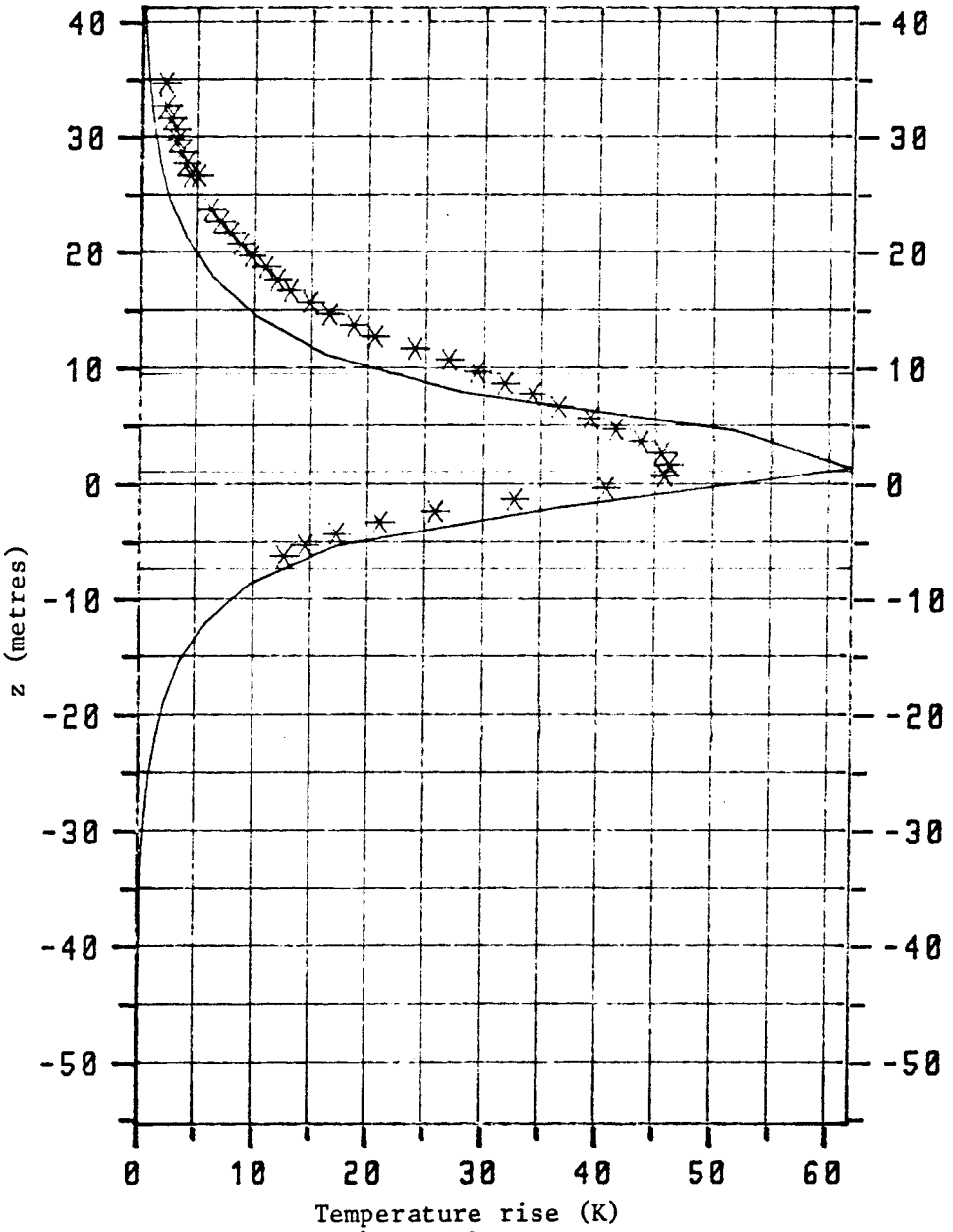

Figure 15.

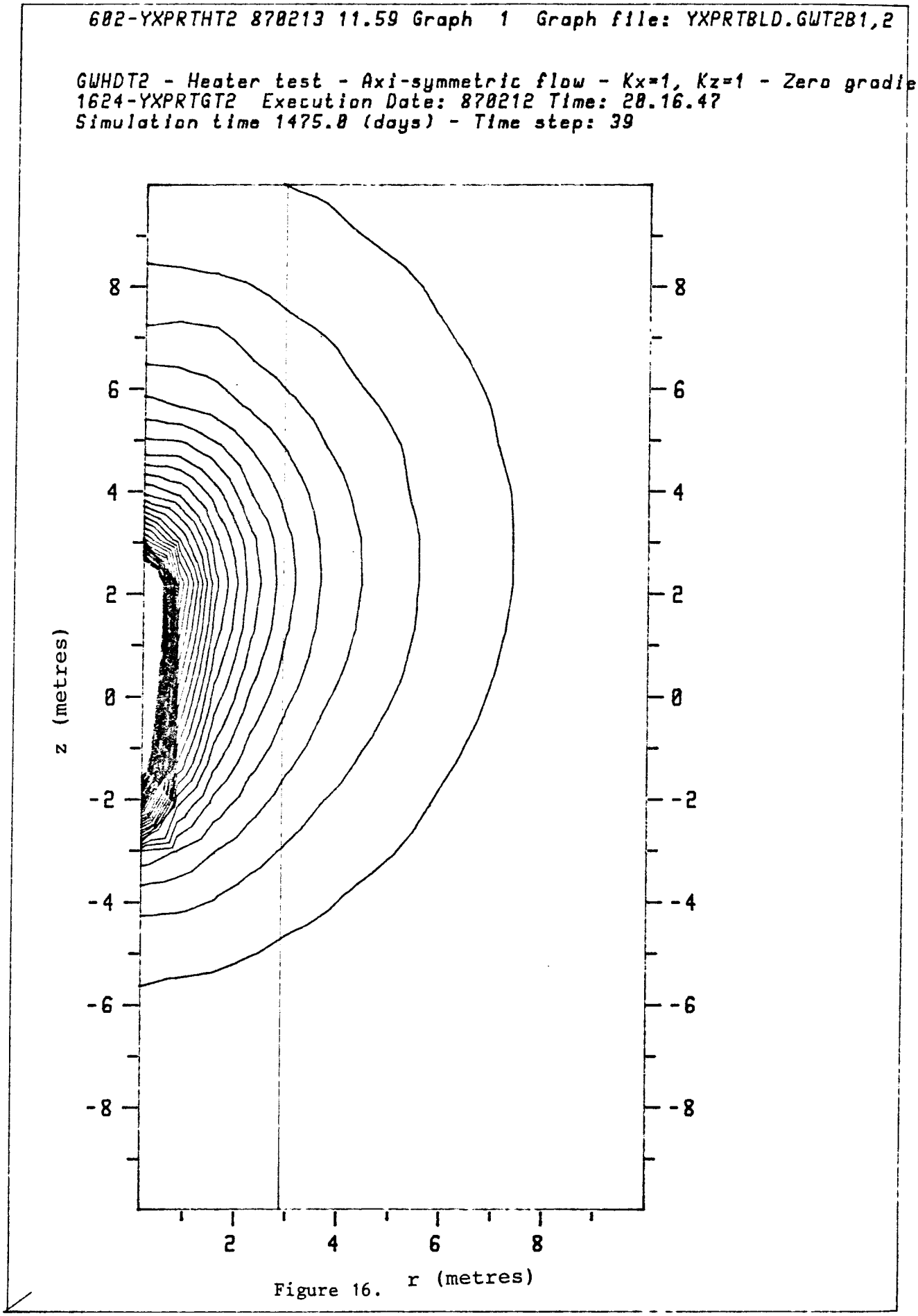
602-YXPRTHT2 870213 11.59 Graph 1 Graph file: YXPRTBLD.GWT2B1,2
GWHDT2 - Heater test - Axi-symmetric flow - Kx=1, Kz=1 - Zero gradient -
1624-YXPRTGT2 Execution Date: 870212 Time: 20.16.47
Simulation time 1475.0 (days) - Time step: 39
z (metres)
8
6
4
2
0
-2
-4
-6
-8
2
4
6
8
r (metres)

Figure 16.

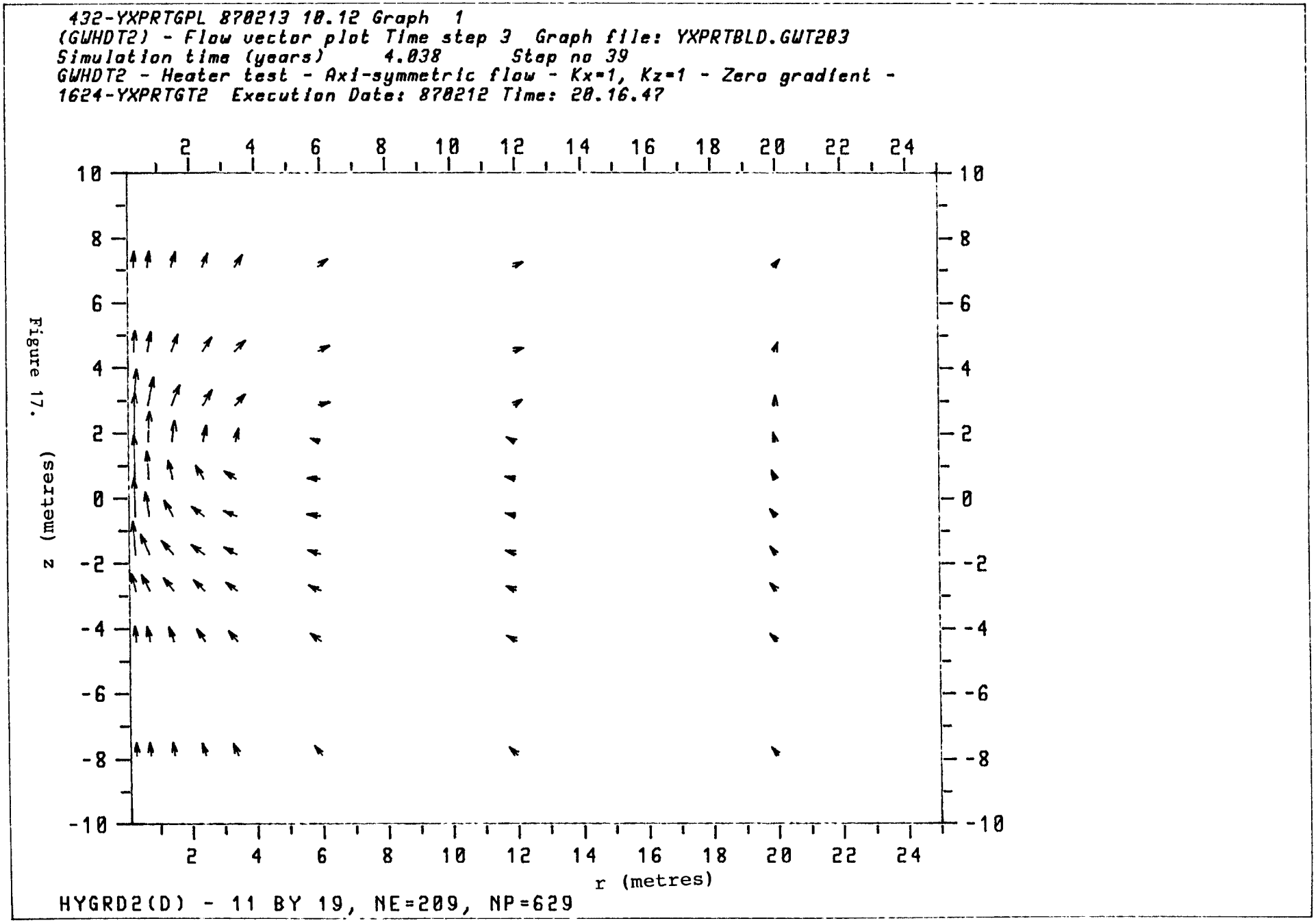
432-YXPRTGPL 870213 10.12 Graph 1
(GWHDT2) - Flow vector plot Time step 3 Graph file: YXPRTBLD.GUT2B3
Simulation time (years) 4.038 Step no 39
GWHDT2 - Heater test - Axi-symmetric flow - Kx=1, Kz=1 - Zero gradient -
1624-YXPRTGT2 Execution Date: 870212 Time: 20.16.47
2 4 6 8 10 12 14 16 18 20 22 24
10 8 6 4 2 0 -2 -4 -6 -8 -10
z (metres)
r (metres)
HYGRD2(D) - 11 BY 19, NE=209, NP=629

Figure 17.

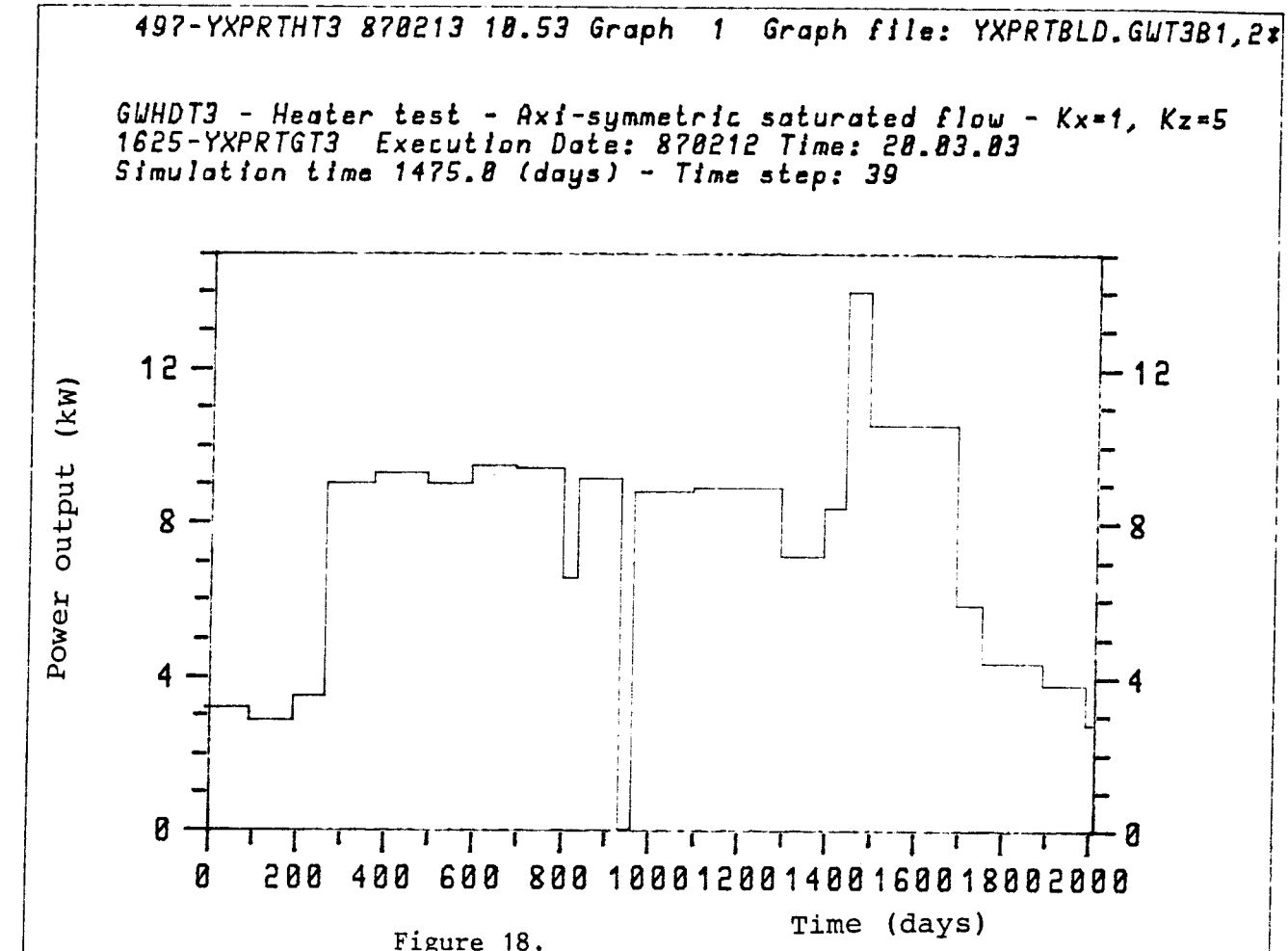

Figure 18.

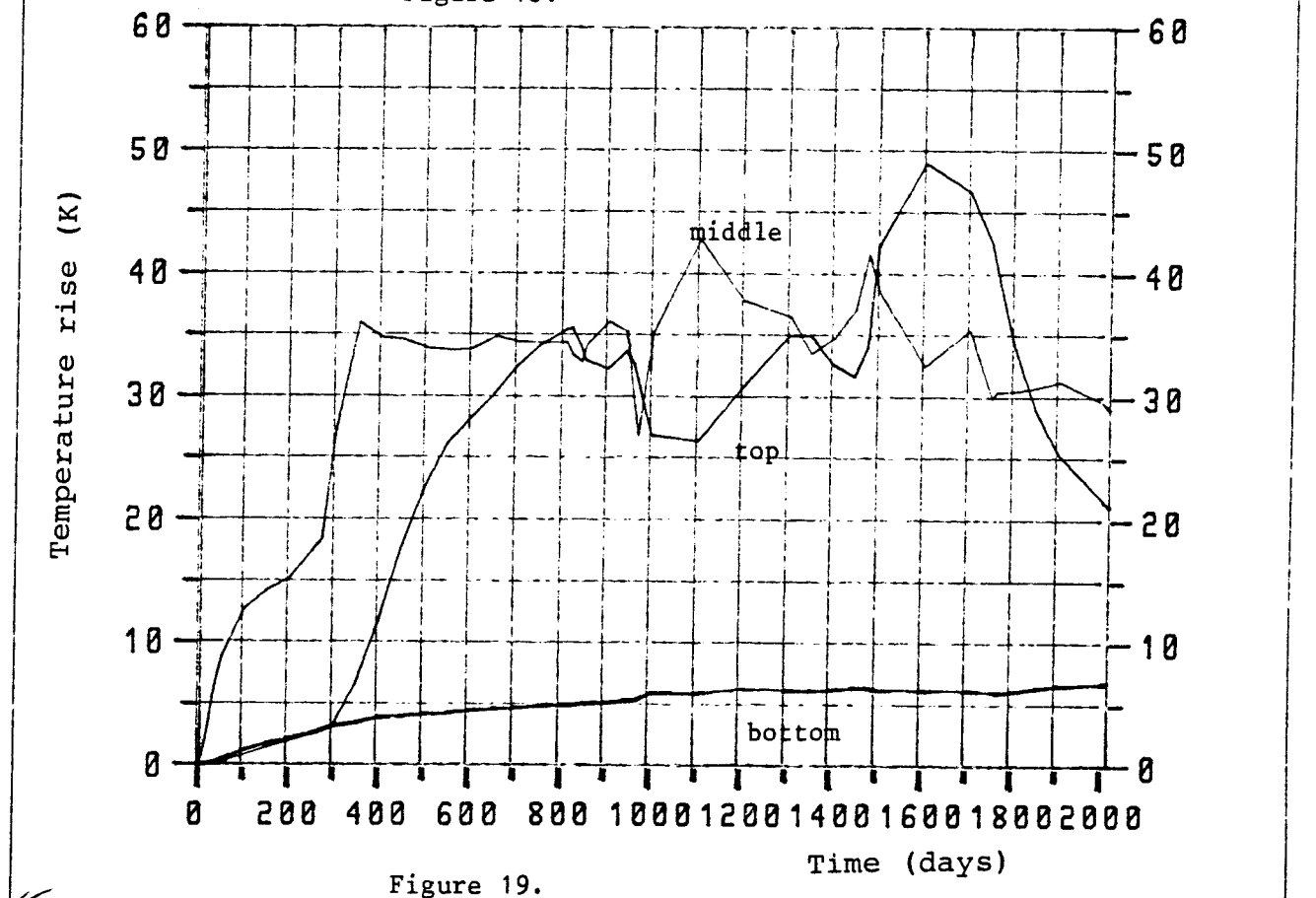

Figure 19.

606-YXPRTHT3 870213 12.03 Graph 1 Graph file: YXPRTBLD.GWT3B1,2

GWHDT3 - Heater test - Axi-symmetric saturated flow - Kx=1, Kz=5
1625-YXPRTGT3 Execution Date: 870212 Time: 20.03.03
Simulation time 1475.0 (days) - Time step: 39

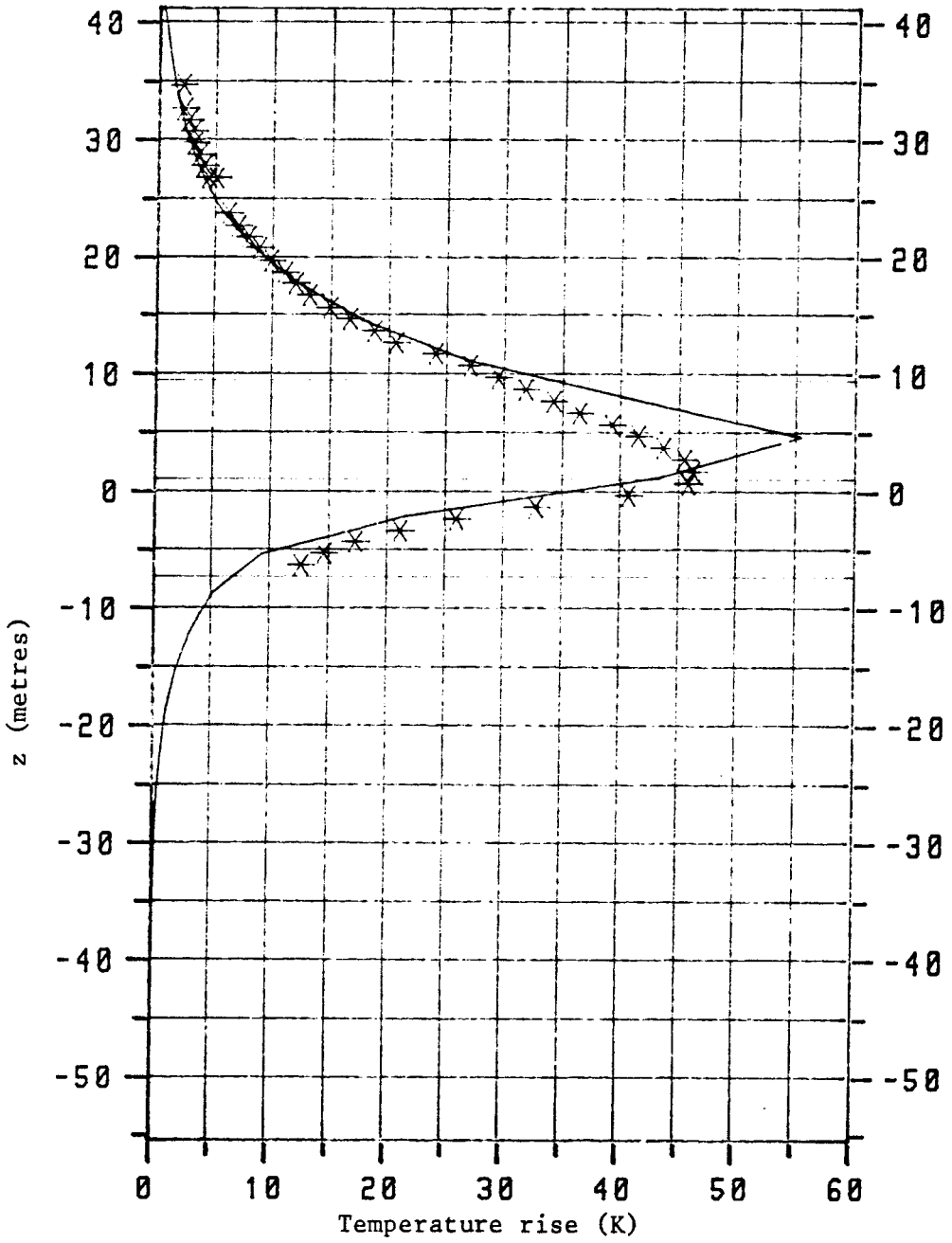

Figure 20.

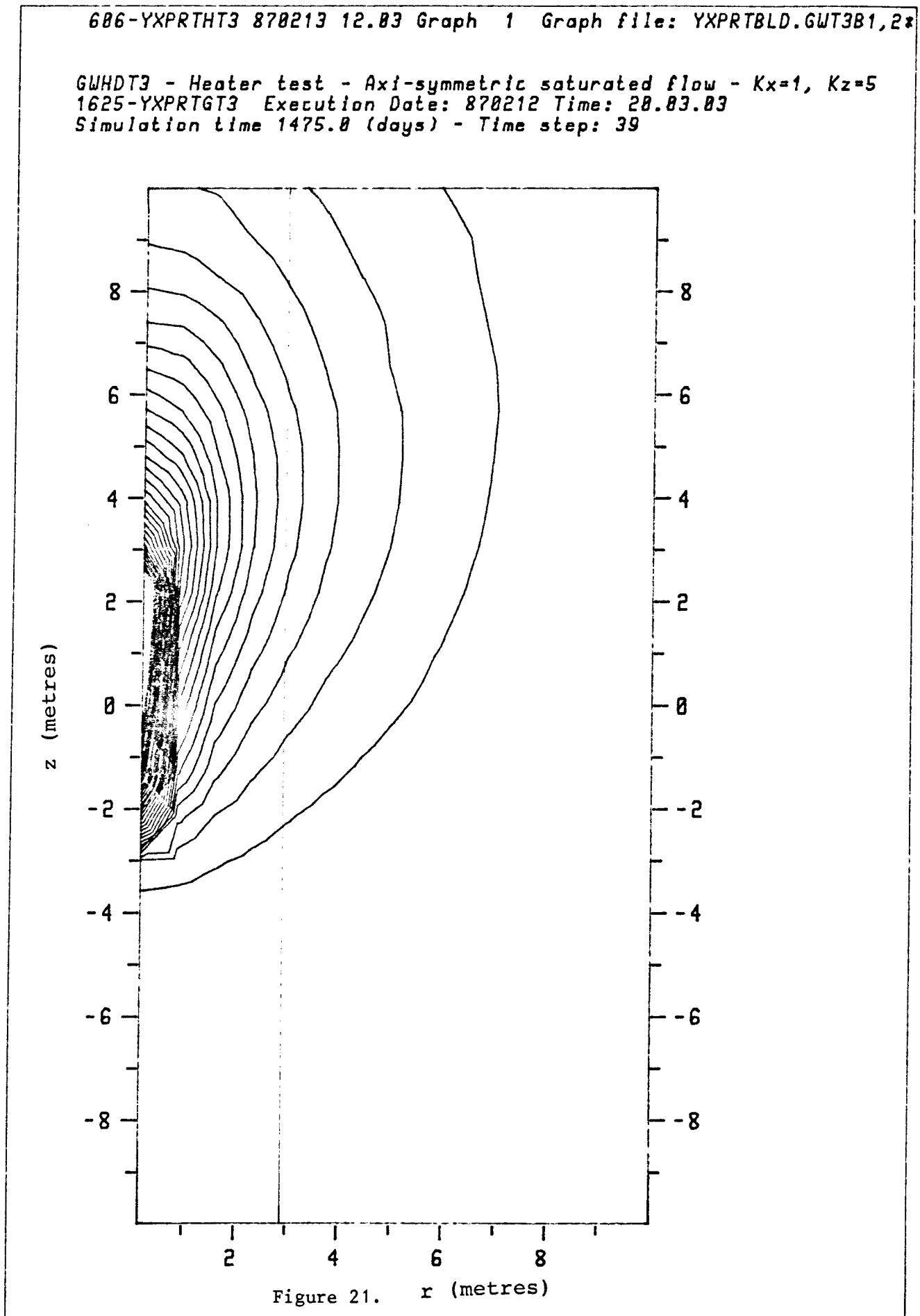
606-YXPRTHT3 870213 12.03 Graph 1 Graph file: YXPRTBLD.GWT3B1,2
GWHDT3 - Heater test - Axi-symmetric saturated flow - Kx=1, Kz=5
1625-YXPRTGT3 Execution Date: 870212 Time: 20.03.03
Simulation time 1475.0 (days) - Time step: 39
z (metres)
8
6
4
2
0
-2
-4
-6
-8
2
4
6
8
r (metres)

Figure 21.

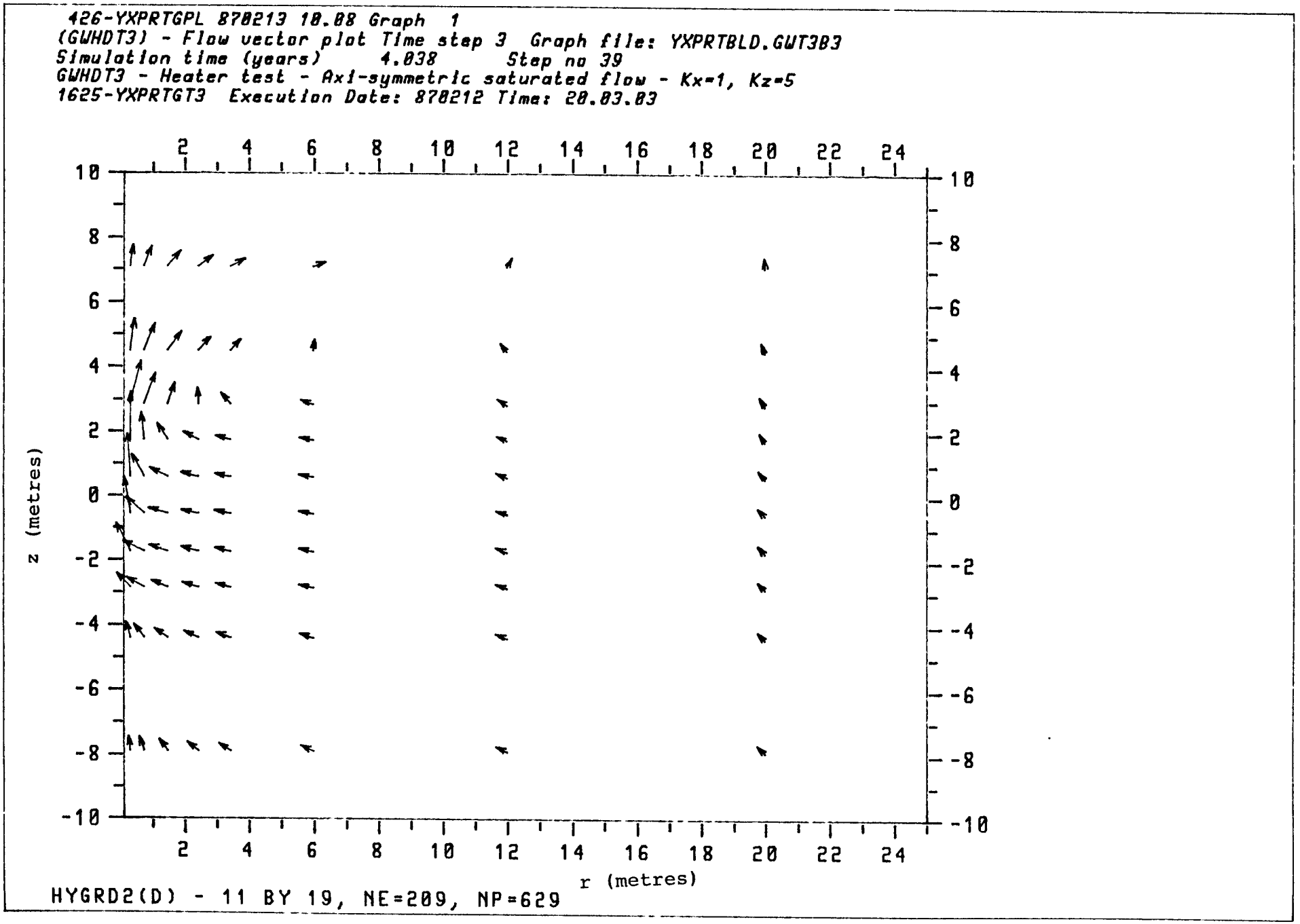
426-YXPRTGPL 870213 10.08 Graph 1
(GWHDT3) - Flow vector plot Time step 3 Graph file: YXPRTBLD.GWT3B3
Simulation time (years) 4.038 Step no 39
GWHDT3 - Heater test - Axi-symmetric saturated flow - Kx=1, Kz=5
1625-YXPRTGT3 Execution Date: 870212 Time: 20.03.03
z (metres)
r (metres)
HYGRD2(D) - 11 BY 19, NE=209, NP=629

Figure 22.

985-YXPRTHI3 870210 14.26 Graph 1 Graph file: YXPRTBLD.HFINB5,6

GWHDR3R1 - Heater test - Axi-symmetric saturated flow - Kx=1, Kz=5
1337-YXPRTGD3 Execution Date: 870209 Time: 13.23.52
Simulation time 1475.8 (days) - Time step: 39

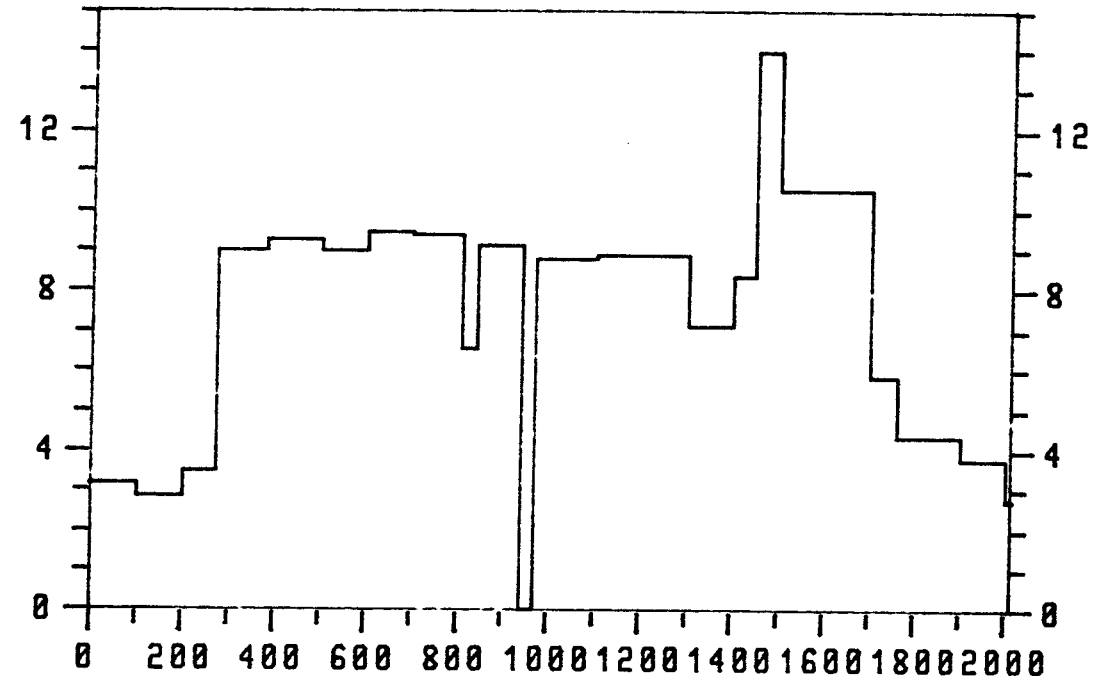

Figure 23. Time (days)

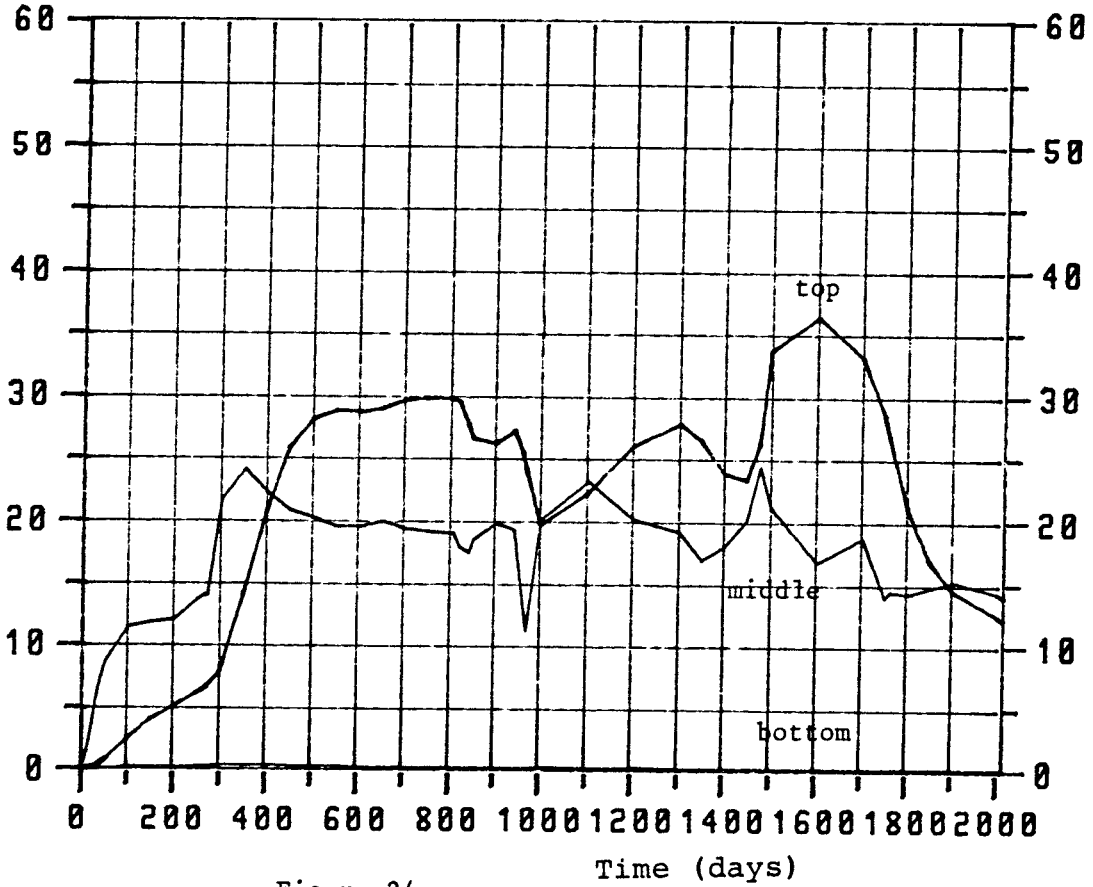

Figure 24.

985-YXPRTHI3 870210 14.26 Graph 1 Graph file: YXPRTBLD.HFINB5,6

GWHDR3R1 - Heater test - Axi-symmetric saturated flow - Kx=1, Kz=5
1337-YXPRTGD3 Execution Date: 870209 Time: 13.23.52
Simulation time 1475.0 (days) - Time step: 39

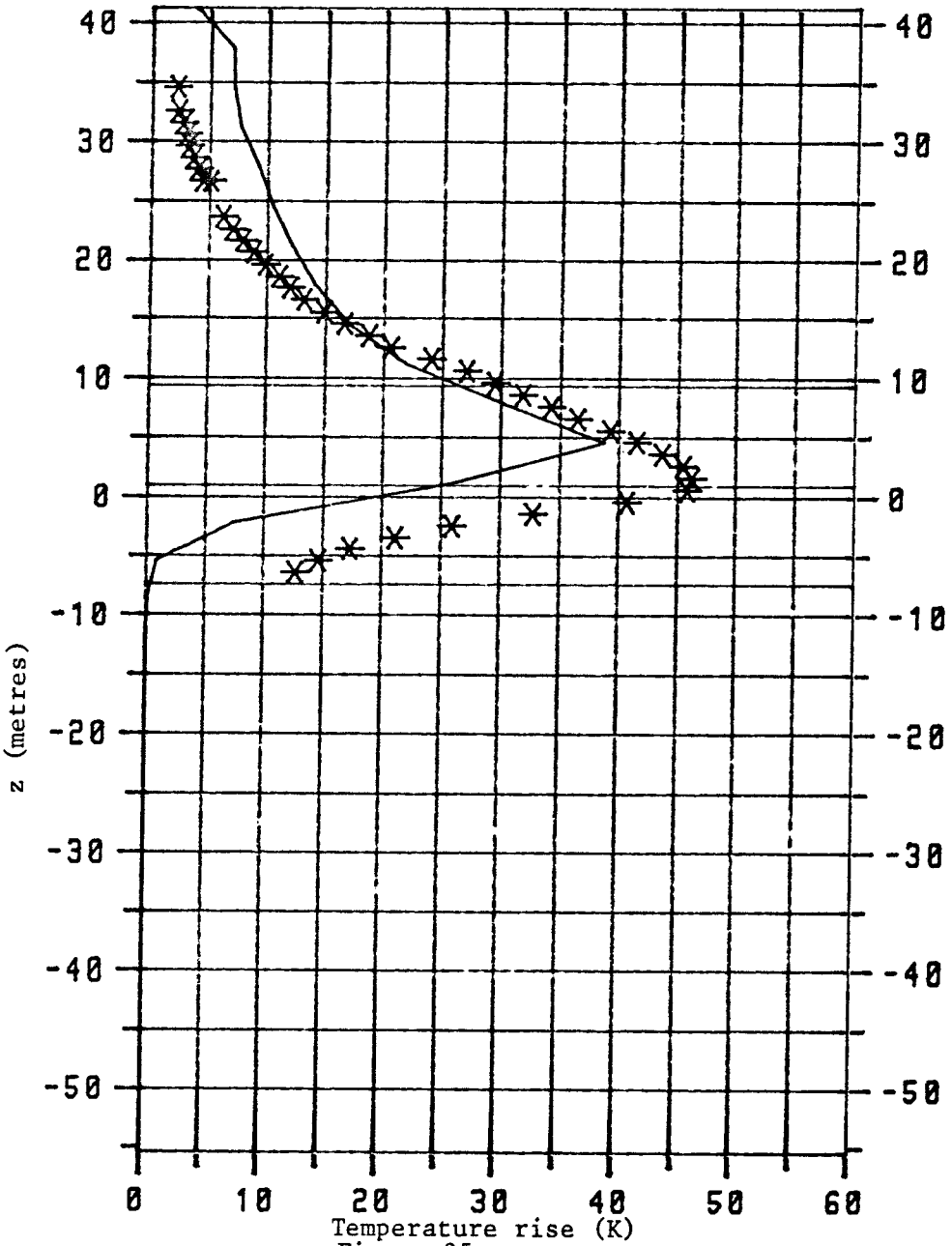

Figure 25.

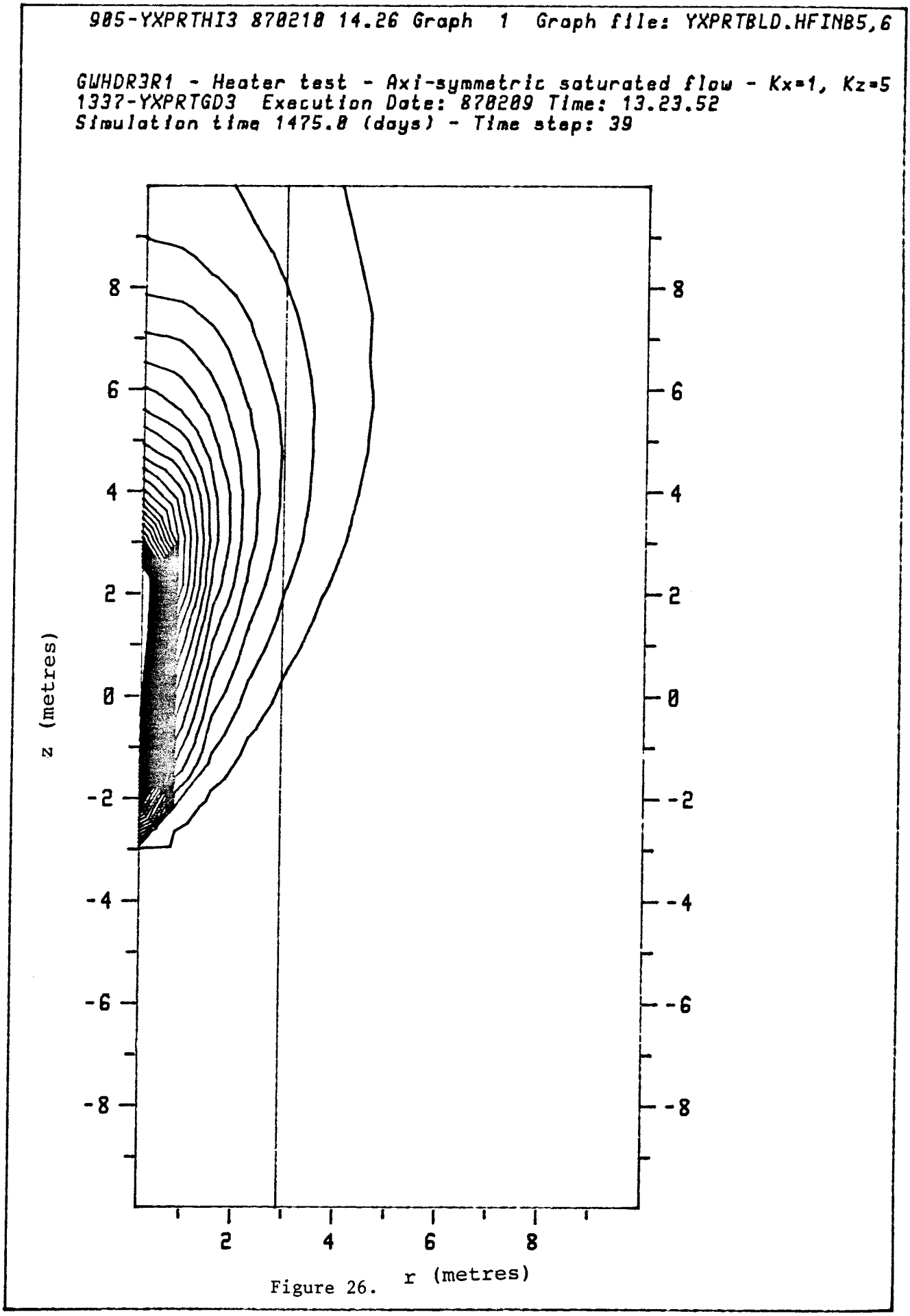
985-YXPRTHI3 870210 14.26 Graph 1 Graph file: YXPRTBLD.HFINB5,6
GWHDR3R1 - Heater test - Axi-symmetric saturated flow - Kx=1, Kz=5
1337-YXPRTGD3 Execution Date: 870209 Time: 13.23.52
Simulation time 1475.0 (days) - Time step: 39
z (metres)
r (metres)
8
6
4
2
0
-2
-4
-6
-8
2
4
6
8

Figure 26.

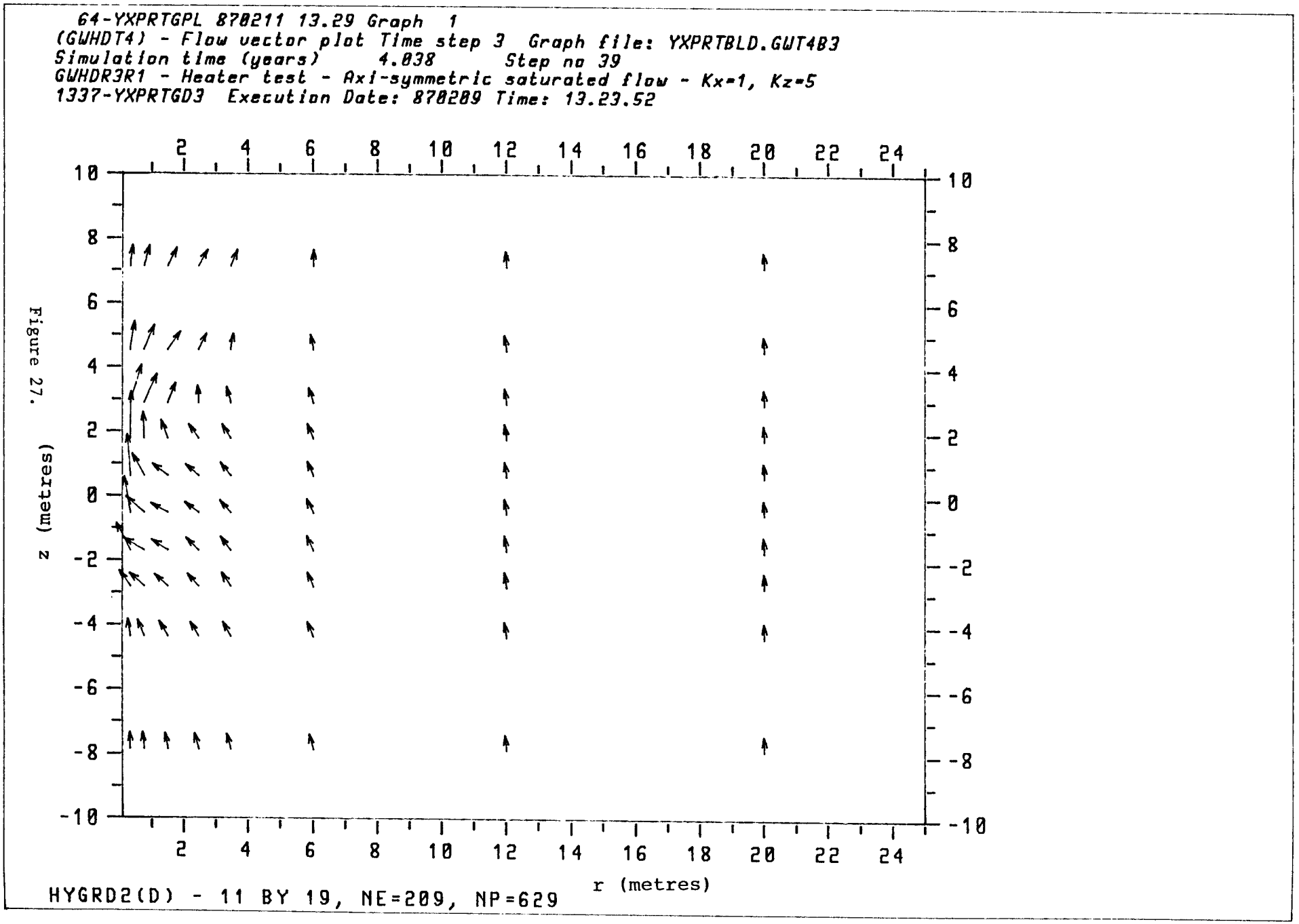
64-YXPRTGPL 870211 13.29 Graph 1
(GWHDT4) - Flow vector plot Time step 3 Graph file: YXPRTBLD.GWT4B3
Simulation time (years) 4.038 Step no 39
GWHDR3R1 - Heater test - Axi-symmetric saturated flow - Kx=1, Kz=5
1337-YXPRTGD3 Execution Date: 870209 Time: 13.23.52
2 4 6 8 10 12 14 16 18 20 22 24
10 8 6 4 2 0 -2 -4 -6 -8 -10
z (metres)
r (metres)
HYGRD2(D) - 11 BY 19, NE=209, NP=629

Figure 27.

List of SKB reports

Annual Reports

1977–78
TR 121
KBS Technical Reports 1 – 120.
Summaries. Stockholm, May 1979.

1979
TR 79–28
The KBS Annual Report 1979.
KBS Technical Reports 79-01 – 79-27.
Summaries. Stockholm, March 1980.

1980
TR 80–26
The KBS Annual Report 1980.
KBS Technical Reports 80-01 – 80-25.
Summaries. Stockholm, March 1981.

1981
TR 81–17
The KBS Annual Report 1981.
KBS Technical Reports 81-01 – 81-16.
Summaries. Stockholm, April 1982.

1982
TR 82–28
The KBS Annual Report 1982.
KBS Technical Reports 82-01 – 82-27.
Summaries. Stockholm, July 1983.

1983
TR 83–77
The KBS Annual Report 1983.
KBS Technical Reports 83-01 – 83-76
Summaries. Stockholm, June 1984.

1984
TR 85–01
Annual Research and Development Report 1984
Including Summaries of Technical Reports Issued during 1984. (Technical Reports 84-01–84-19)
Stockholm June 1985.

1985
TR 85-20
Annual Research and Development Report 1985
Including Summaries of Technical Reports Issued during 1985. (Technical Reports 85-01-85-19)
Stockholm May 1986.

1986
TR86-31
SKB Annual Report 1986
Including Summaries of Technical Reports Issued during 1986
Stockholm, May 1987

Technical Reports

1987

TR 87-01
Radar measurements performed at the Klipperås study site
Seje Carlsten, Olle Olsson, Stefan Sehlstedt, Leif Stenberg
Swedish Geological Co, Uppsala/Luleå
February 1987

TR 87-02
Fuel rod D07/B15 from Ringhals 2 PWR: Source material for corrosion/leach tests in groundwater
Fuel rod/pellet characterization program part one
Roy Forsyth
Studsvik Energiteknik AB, Nyköping
March 1987

TR 87-03
Calculations on HYDROCOIN level 1 using the GWHRT flow model
Case 1 Transient flow of water from a borehole penetrating a confined aquifer
Case 3 Saturated-unsaturated flow through a layered sequence of sedimentary rocks
Case 4 Transient thermal convection in a saturated medium
Roger Thunvik, Royal Institute of Technology, Stockholm
March 1987